MOLECULAR AND CELLULAR BIOLOGY, May 2011, p. 2134–2150 Vol. 31, No. 10
0270-7306/11/$12.00 doi:10.1128/MCB.05051-11

Motor Protein Myo1c Is a Podocyte Protein That Facilitates the Transport of Slit Diaphragm Protein Neph1 to the Podocyte Membrane▽

E. Arif,[1] M. C. Wagner,[2] D. B. Johnstone,[1] H. N. Wong,[1] B. George,[1] P. A. Pruthi,[4] M. J. Lazzara,[3] and D. Nihalani[1]*

Department of Medicine, Renal Electrolyte and Hypertension Division, University of Pennsylvania, Philadelphia, Pennsylvania 19104[1]; Department of Medicine, Division of Nephrology, Indiana University, Indianapolis, Indiana 46202[2]; Department of Chemical and Biomolecular Engineering, University of Pennsylvania, Philadelphia, Pennsylvania 19104[3]; and Biotechnology and Management of Bioresources Division, The Energy and Resources Institute, New Delhi 110003, India[4]

Received 11 January 2011/Returned for modification 3 February 2011/Accepted 2 March 2011

The podocyte proteins Neph1 and nephrin organize a signaling complex at the podocyte cell membrane that forms the structural framework for a functional glomerular filtration barrier. Mechanisms regulating the movement of these proteins to and from the membrane are currently unknown. This study identifies a novel interaction between Neph1 and the motor protein Myo1c, where Myo1c plays an active role in targeting Neph1 to the podocyte cell membrane. Using *in vivo* and *in vitro* experiments, we provide data supporting a direct interaction between Neph1 and Myo1c which is dynamic and actin dependent. Unlike wild-type Myo1c, the membrane localization of Neph1 was significantly reduced in podocytes expressing dominant negative Myo1c. In addition, Neph1 failed to localize at the podocyte cell membrane and cell junctions in Myo1c-depleted podocytes. We further demonstrate that similarly to Neph1, Myo1c also binds nephrin and reduces its localization at the podocyte cell membrane. A functional analysis of Myo1c knockdown cells showed defects in cell migration, as determined by a wound assay. In addition, the ability to form tight junctions was impaired in Myo1c knockdown cells, as determined by transepithelial electric resistance (TER) and bovine serum albumin (BSA) permeability assays. These results identify a novel Myo1c-dependent molecular mechanism that mediates the dynamic organization of Neph1 and nephrin at the slit diaphragm and is critical for podocyte function.

Glomerular filtration assembly involves three layers, a fenestrated endothelium, a glomerular basement membrane, and specialized epithelial cells termed podocytes. Studies of various glomerular diseases, including nephrotic syndromes, diabetic nephropathy, and focal segmental glomerulosclerosis (FSGS), suggest that podocytes are a major target of these insults and that their dysfunction is associated with proteinuria and decreased kidney function. The identification of podocyte proteins such as nephrin, Neph1, podocin, synaptopodin, CD2AP, and α-actinin-4 that are localized specifically at the podocyte filtration barrier or slit diaphragm has provided greater insight into the mechanisms that mediate podocyte structure and function. Recent analyses of various glomerular disorders, including FSGS, membranous nephropathy, and minimal-change nephrotic syndrome, have reported alterations in the expression and localization of the slit diaphragm proteins nephrin, podocin, CD2ap, and Neph1 (20, 45). These data provide further support for the hypothesis that alterations in the molecular arrangement of the slit diaphragm contribute to the development of proteinuria in several glomerular diseases.

In contrast to nephrin, Neph1 is widely expressed in numerous cell types, including podocytes, where it localizes at the insertion site of the slit diaphragm (2, 11). Structurally, the extracellular region of Neph1 contains five immunoglobulin-like repeats, followed by a transmembrane domain and a cytoplasmic domain of ~198 to 235 amino acids (40). Knockout studies with mice suggested that similar to nephrin, the genetic deletion of Neph1 results in a podocyte effacement phenotype with proteinuria and early postnatal death (7). These similarities and the ability of these proteins to interact at extracellular and intracellular regions have prompted investigators to propose a model where nephrin and Neph1 form a structural framework for the slit diaphragm (44). A recently reported biochemical analysis of Neph1 phosphorylation and its interaction with nephrin has provided insight into the functional role of this complex in maintaining podocyte structure and function (10). Interactions mediated by the cytoplasmic domains of Neph1 and nephrin with various actin-associated proteins, including CD2AP, ZO-1, CASK, IQGAP1, β-arrestin, Nck, Grb2, α-actinin 4, Synaptopodin, and the polarity proteins Par3 and Par6, suggest their role in transducing signals that induce actin polymerization in podocytes (35, 37, 44). An understanding of how these interactions are regulated and functionally involved in maintaining the integrity of the slit diaphragm has been the subject of many recent investigations (10, 44, 45).

* Corresponding author. Mailing address: Department of Medicine, Renal Electrolyte and Hypertension Division, University of Pennsylvania, Philadelphia, PA 19104. Phone: (215) 898-0192. Fax: (215) 898-0189. E-mail: deepakn@mail.med.upenn.edu.

▽ Published ahead of print on 14 March 2011.

Recent evidence from various *in vitro* and *in vivo* studies suggests that foot processes of podocytes respond dynamically to glomerular injury by regulating their associated protein complexes, thus resulting in a reorganization of the actin cytoskeleton (4, 37, 41, 44, 48). Therefore, it is likely that glomerular injury affects the interactions and distribution of slit diaphragm proteins, resulting in the loss of the slit diaphragm structure. These studies suggest that regaining glomerular function following injury will require the retargeting of these proteins back to their physiological locations in the cell. Indeed, our recent results and results from other investigators demonstrated a loss of the interaction between Neph1, nephrin, and ZO-1 in response to glomerular injury and a redistribution of the Neph1 complex from the podocyte cell membrane to the cell cytoplasm (8, 34, 47, 49). Consistent with our hypothesis, the Neph1-nephrin complex was rapidly restored to the cell membrane during recovery. These results support the hypothesis that this complex is regulated in a dynamic fashion but do not explain the mechanism by which these proteins are targeted to the cell membrane.

In this study, we identify a novel interaction between Neph1 and the motor protein Myo1c. Myo1c is a member of the class I myosins that belong to the family of unconventional myosins (13). There are 9 human myosin I genes identified, with many cells expressing more than one myosin isoform (12). They all are single headed with a short, highly basic, carboxy-terminal tail domain that can bind to acidic phospholipids (6, 43). The head domain, also known as the motor domain, contains ATP and actin binding sites (3). In addition, all mammalian myosin I family members have a middle or neck domain composed of 2 to 6 IQ motifs that bind calmodulin (1). Members of this family are widely expressed, are generally associated with membrane structures, and are found in actin-rich cortical structures such as filopodia, lamellipodia, and ruffles and in the leading edges of migrating cells (3). Myosin I family members have been implicated in multiple cellular processes occurring at the cell membrane, including endocytosis, vesicle trafficking, and ion channel regulation and regulating membrane dynamics and structure in nearly all eukaryotic cells (9, 16, 28). Immunofluorescence microscopic studies of various cell types demonstrated the presence of Myo1c at the cell periphery and plasma membrane, particularly at the leading edges of motile cells (46). Studies of hair cells support an F-actin-mediated role for Myo1c in the regulation of a channel located in the stereocilia of these sensory cells (14, 17). Data from recent reports also support a role for Myo1c as a protein translocator that mediates the delivery of GLUT4 (glucose transporter type 4) vesicles to the plasma membrane in adipocytes (5) and the intracellular trafficking of NEMO (NF-κB essential modulator) (30). Results presented in this study further demonstrate that Myo1c plays a critical role in the translocation of Neph1 complexes in podocytes. Myo1c's ability to interact with membranes, F-actin, Neph1, and nephrin supports our hypothesis that this motor protein actively contributes to the dynamic organization of the filtration slit.

MATERIALS AND METHODS

Antibodies and reagents. Monoclonal purified antibody (Ab) to Myo1c and polyclonal purified antibody to Neph1, nephrin, Myo1b, Myo1e, and Myo1d were previously described (2, 46). Other antibodies, including ZO-1 monoclonal and polyclonal antibodies (Invitrogen), anti-phosphotyrosine mouse monoclonal antibody (P-Tyr-100; Cell Signaling), caveolin 1 polyclonal antibody (Abcam), transferrin receptor monoclonal antibody (Abcam), podocin antibody (Cell Signaling), and CD16 monoclonal antibody (Immunotech), were purchased commercially. The fluorophore secondary antibodies Alexa Fluor 488 goat anti-rabbit IgG(H+L) (catalogue number A-11008; Invitrogen), Alexa Fluor 568 goat anti-mouse IgG(H+L) (catalogue number A-11004; Invitrogen), Alexa Fluor 647 goat anti-rabbit IgG(H+L) (catalogue number A-21244; Invitrogen), Alexa Fluor 350 goat anti-mouse (catalogue number A-21093; Invitrogen), Alexa Fluor phalloidin (catalogue number A12379; Invitrogen), and wheat germ agglutinin (WGA) Alexa Fluor 594 conjugate (catalogue number W11262; Invitrogen) were commercially obtained. The cell transfection reagents purchased were an Amaxa Nucleofector kit (catalogue number VCA 1003; Lonza), FuGENE HD (catalogue number 04709691001; Roche Applied Science), and Lipofectamine 2000 (catalogue number 11668-019; Invitrogen). All chemical reagents were obtained commercially from Sigma and Calbiochem.

Plasmids and shRNA. Vector pBABE-puro was obtained from Addgene. Mammalian expression plasmids encoding green fluorescent protein (GFP)-tagged full-length Myo1c and mutant Myo1c without the head and IQ domains were obtained as described previously (47) and through generous collaboration with Mike Ostap. Myo1c small hairpin RNA (shRNA) plasmids and lentiviruses expressing Myo1c and Neph1 shRNA were commercially purchased from Sigma (Myo1c catalogue number NM_033375; Neph1 catalogue number NM_018240). The transfection of shRNA plasmids was performed by electroporation using Amaxa reagent. Briefly, podocytes (1×10^6 cells) were suspended in 100 μl of Nucleofector solution provided with the Amaxa transfection reagent (Lonza) with 5 μg of shRNA, and transfection was performed by electroporation using the X-100 program of the Amaxa electroporator (Lonza). Transfected cells were grown in 2.5 μg/ml puromycin-containing medium for the selection of stable transfectants. Transfection with Lipofectamine 2000 (Invitrogen) was performed according to the manufacturer's protocol. CD16-Neph1, His-Neph1CD, glutathione *S*-transferase (GST)-Neph1CD, FLAG-Neph1, and GST-nephrin constructs were previously described (45).

Cell culture. The human podocyte cell line was cultured in RPMI 1640-based medium supplemented with 10% fetal bovine serum (FBS) (Invitrogen), 2 g/liter of sodium bicarbonate ($NaHCO_3$), insulin-transferrin-selenium (ITS) supplement (Sigma-Aldrich), and 200 units/ml penicillin and streptomycin (Roche Applied Science), as described previously (47). The podocyte cells were grown in collagen-coated culture dishes at 33°C and 5% CO_2. Podocytes were differentiated by thermoswitching to 37°C as described previously (47). COS-7 cells were cultured in Dulbecco's modified Eagle's medium (DMEM) supplemented with 10% fetal bovine serum (Invitrogen) and 200 units/ml penicillin and streptomycin (Roche Applied Science). Transfection was performed with Amaxa Nucleofector devices and reagents by electroporation. Transfection with Lipofectamine 2000 (Invitrogen) and Fugene-6 (Roche Applied Science) was performed according to the manufacturers' protocols.

Generation of podocytes overexpressing Neph1. Neph1 was cloned into the pBABE vector (Addgene) by using standard PCR techniques at EcoRI and SalI sites. Retroviruses overexpressing Neph1 were generated by the transfection of this cDNA into Phoenix cells according to the manufacturer's instructions. Ten milliliters of DMEM was added after 4 h of transfection, and after 18 to 24 h of transfection, supernatants containing the retrovirus with the Neph1 construct were collected and filtered with a 0.22-μm filter. Target podocytes were grown up to subconfluent levels, and the podocyte cells were infected with viral particles three times over a period of 36 h. Infections were made twice a day after a gap of 6 h, and a third infection was given after 18 to 24 h. After 6 h of the third infection, cells were washed three times with 1× phosphate-buffered saline (PBS), and normal RPMI medium was added to these cells. Stably transfected cells overexpressing Neph1 were selected by using puromycin as a selection marker. Podocyte cells overexpressing Neph1 from a total of 20 100-cm^2 culture dishes were used for proteomic experiments, and lysates were obtained by using radioimmunoprecipitation assay (RIPA) buffer.

Isolation of Neph1 complexes. GST-Neph1-antibody and preimmunized serum affinity columns were prepared by using *N*-hydroxysuccinimide (NHS)-activated Sepharose 4 Flow Fast (GE Healthcare) according to the manufacturer's instructions. The Neph1-overexpressing podocyte lysate was loaded onto each column. Both Neph1-antibody and control columns were washed and eluted with glycine HCl buffer (pH 2.5). The eluate was neutralized with Tris (pH 8.0), and all eluates were later concentrated using a 10-kDa-cutoff centrifugal filter (Millipore). The concentrated protein from the Neph1-antibody and control columns was separated by sodium dodecyl sulfate (SDS)-PAGE. Differentially visible bands were excised from the gel and submitted for tandem mass spec-

trometry (MS-MS) analysis at the proteomics core facility of the University of Pennsylvania.

Glomerular isolation. Rat and mouse glomeruli were isolated by graded sieving as described elsewhere previously (18). The average purity of the rat glomerular preparations was 80 to 90%, and that of the mouse preparations was 60 to 70%. Glomeruli were resuspended at a concentration of 10,000 glomeruli/ml in extraction buffer (RIPA buffer).

Reverse transcription-PCR. Reverse transcription (RT)-PCR of the human podocyte cells was performed by using specific primers designed as well as those reported elsewhere previously. The following primers were used: forward primer 5′-GGGTGAAGAGATCAGCCATC-3′ and reverse primer 5′-CTTATTGTCC GCACGCTGTA3-′ for Myo1c, forward primer 5′-AGAGCCAATGCTGGAA AGAA-3′ and reverse primer 5′-TTGTGCGATAGAGCTTGGTG-3′ for Myo1b, forward primer 5′-CAAAAGAACCAAGGCAGCTC-3′ and reverse primer 5′-TT CACCAGCACTCCAACAAG-3′ for Myo1d, and forward primer 5′-AGCAAAG CGTTACGAGGAGA-3′ and reverse primer 5′-TACAAAGCCTTGCACTGTG G-3′ for Myo1e, giving products of 695, 658, 699, and 609 bp, respectively. Primer details for Myo1V and MyoVI were reported previously (23, 42).

Immunoprecipitation and immunoblotting. Detailed procedures for immunoprecipitation and immunoblotting experiments were described elsewhere previously (10, 32, 47). Endogenous Neph1 and Myo1c were extracted from podocytes and glomeruli in RIPA buffer (phosphate-buffered 0.9% NaCl [PBS] containing 0.1% SDS, 1% Nonidet P-40, and 0.5% sodium deoxycholate). The Phoenix cells for the preparation of retroviruses containing Neph1 cDNA were cultured in DMEM supplemented with 10% fetal bovine serum (Invitrogen) and 200 units/ml penicillin and streptomycin (Roche Applied Science).

Pulldown. Recombinant proteins, His-Neph1, GST-Neph1, and GST-nephrin, were expressed and purified from *Escherichia coli* BL21 cells (Stratagene). Five micrograms of each fusion protein was separately mixed with purified recombinant full-length Myo1c (2 μg) produced in a baculovirus expression system (a kind gift from Michael Ostap). The Neph1/nephrin complexes were pulled down using Neph1 antibody and/or GST-agarose. After washing with PBS containing 0.1% Tween 20, protein complexes were eluted with SDS sample buffer and resolved by SDS-PAGE prior to immunoblotting with the indicated antibodies.

Lipid raft preparation. Lipid rafts were prepared from podocyte and mouse glomerulus lysates according to a method described previously (2). Podocytes and mouse glomeruli were lysed in cold Triton X-100 buffer containing 0.25% Triton X-100 (1% in the case of glomeruli), 150 mM NaCl, 1 mM EGTA, and 25 mM Tris-HCl (pH 7.4) with protease and phosphatase inhibitors. A solution of a different density was prepared by using Optiprep density gradient medium (catalogue number D1556; Sigma). In an ultracentrifuge tube, 0.67 ml of cell lysate and 1.33 ml of 60% Optiprep were mixed by pipetting to obtain a final density of 40%. A total of 2.0 ml of 30% gradient Optiprep solution at the top of above-described solution and then 1.0 ml of 5% gradient Optiprep solution were carefully added, making a total of three layers. Tubes were ultracentrifuged at 45,000 rpm using a Beckman SW 55Ti rotor (Sorvall Discovery 90SE; Hitachi) at 4°C for a period of 3.5 to 4.0 h. The Triton X-100-insoluble lipid raft layer was identifiable at the interface between the 5 and 30% Optiprep solutions. Top-to-bottom 1-ml fractions were sequentially collected into separate tubes.

Cell treatment. Podocytes were grown to confluence, and cells were then serum starved for a period of 4 h. After serum starvation, cells were treated with either normal RPMI medium, 5 mM latrunculin B (catalogue number BML-T110-0001; Enzo Life Science), or 30 μM nocodazole (catalogue number M1404; Sigma) for 1 h. Cells were washed twice with PBS (1×) and then fixed with 4% paraformaldehyde (PFA) (in 1× PBS). For puromycin aminonucleoside (PAN) treatment, cultured podocytes were grown to 80 to 90% confluence and treated with 100 μg/ml PAN (Sigma) for 1 h. Recovery was induced by washing cells with growth medium and incubating the cells in it for 1 h.

Animals and acute renal ischemia. Male Sprague-Dawley rats were obtained from Harlan Labs (Indianapolis, IN). All experiments were conducted in accordance with NIH guidelines and approved by the Institutional Animal Care and Use Committee. Ischemia was performed as described previously (47).

Immunogold electron microscopy. The preparation of samples was performed by using standard methods described previously (2). Adult rats were perfused with 4% formaldehyde, and kidneys were isolated and submitted to the Biomedical Imaging Core/Electron Microscopy Resource Laboratory, University of Pennsylvania, for immunogold analysis.

Indirect immunofluorescence microscopy. Podocytes were grown on coverslips and fixed with 4% paraformaldehyde (in 1× PBS), followed by permeabilization with 0.1% SDS. Myo1c and Neph1 antibodies were diluted to 1:100 in 3% bovine serum albumin (BSA) in 1× PBS. Podocytes were incubated overnight with primary antibodies at 4°C, followed by PBS washes and incubation with secondary antibodies at a dilution of 1:1,000 for 1 h at 37°C. After the PBS washes, the coverslips were mounted by using GelMount. Fluorescence microscopy was performed with a Zeiss wide-field microscope equipped with an Axioplan upright microscope with a Zeiss FluoArc mercury lamp and a Zeiss AxioCam HRm high-resolution monochrome charge-coupled-device (CCD) camera, and 100× and 40× oil immersion objectives were used. AxioVision 4.5 software was used for acquisition and analysis with the microscope. An Olympus 1X70 microscope and the Metamorph imaging system (Universal Imaging Corporation, West Chester, PA) were also used for fluorescence microscopy. Cells were labeled for Myo1c (Alexa 568), F-actin (Alexa 488 phalloidin), and Neph-1 (Alexa 647) using the 488-nm, 568-nm, and 633-nm laser lines of the argon and helium-neon lasers. All parameters were kept constant, including exposure time while taking images. Images were taken in a format of 16 bits. Images were analyzed by using Image J software. The mean pixel intensity and integrated intensity were obtained, keeping the threshold constant in the case of analyses of the whole cell or any particular region of interest (ROI). Regions of interest were selected manually, specially taking the cell boundary, using Image J software. For Pearson's correlation coefficient (*Rr*) determinations, single-image planes were selected. After background subtraction, the Myo1c image was thresholded and used to create a binary mask for analyses of the *Rr*. Regions of interest were selected mainly at the cell boundary. Representative images from a minimum of three experiments are given, and a quantitative analysis was performed on at least eight image fields for each time point. Confocal microscopy imaging was performed with a Nikon TE300 inverted microscope fitted with a Bio-Rad Radiance 2000 MP3 system (Bio-Rad Laboratories, Inc.) on a 60× 1.45-numerical-aperture oil objective.

Immunohistochemistry. Adult rats were perfused with 4% paraformaldehyde in phosphate-buffered saline. Kidneys were removed and washed with cold PBS and fixed in Parafilm wax, from which 40-μm sections were later obtained with a sliding microtome. Procedures for immunohistochemistry were performed according to instructions in the Abcam technical guide, with some modifications. Briefly, tissue sections were deparaffinized and incubated with Tris-EDTA (pH 9.0) buffer for antigen retrieval at 65°C overnight. The sections were rinsed with running water and then blocked with 5% BSA (in 1× Tris-buffered saline [TBS] containing 0.025% Triton X-100) for 1 h at room temperature. Primary antibodies for Myo1c (1:75 dilution), Neph1 (1:50 dilution), and ZO-1 (1:400 dilution) were diluted in 3% bovine serum albumin (in 1× PBS) and incubated overnight at 4°C. The sections were washed with 1× TBS five times and then incubated with Alexa Fluor-labeled secondary antibodies at a dilution of 1:500 for 1 h at 37°C. After 5 washings with TBS (1×), sections were mounted with antifade reagent containing 4′,6-diamidino-2-phenylindole (DAPI) and left overnight in the dark for drying. Sections stained with secondary antibodies alone were used as negative controls.

Podocyte labeling with extracellular Neph1 antibody. Neph1 antibody directed toward the extracellular domain of Neph1 was generated in rabbits by FabGennix, Inc., using a synthesized peptide (TISQLLIEPTDLDIGRVF TC). Podocyte cells on coverslips were fixed with 4% paraformaldehyde and incubated with Neph1 extracellular antibody in 3% BSA (in 1× PBS) overnight at 4°C without permeabilization. Cells were washed with 1× PBS, treated with Alexa Fluor 488 rabbit antibody for 1 h at 37°C, and mounted onto slides for immunofluorescence analysis using epifluorescence and/or confocal microscopy.

CD16 experiment. CD16-Neph1 was transfected into Myo1c knockdown and control human podocyte cells. The CD16 construct was transfected by using Lipofectamine 2000 according to the manufacturer's instructions. Following 36 h of transfection, cells were serum starved for 6 h by incubation in RPMI medium without FBS. After starvation, cells were processed for CD16 staining. The cells were moved to 4°C on ice for 30 min for equilibrium. The CD16 monoclonal antibody (Immunotech) was prepared in ice-cold serum-free RPMI medium at a dilution of 1:100 (of 0.2 mg/ml of stock Ab) and incubated for 30 min at 4°C. After washing, the cells were incubated with Alexa 594 anti-mouse secondary Ab with 1:1,000 dilutions in RPMI medium at 37°C for 30 min. Cells were washed quickly with 1× PBS and then fixed in 4% PFA. Immunofluorescence analysis was performed by using epifluorescence and confocal microscopes.

Wound assay. Control and Myo1c knockdown podocytes were grown under differentiated conditions in 35-mm glass-bottom culture dishes (Mat Tek Corporation) until they reached confluence. At 3 days postconfluence, wounds were created by using a 20-μl sterile pipette tip with two strokes at a 90° angle and washed twice with PBS to remove all the suspended cells in the medium. Hanks balanced salt solution (HBSS) with Ca^{2+}/Mg^{2+} was added immediately to capture the live image. After imaging, HBSS was replaced with fresh complete RMPI medium, and the mixture was incubated further at 37°C for the indicated times. Images were taken at different time points, at 6 h, 9 h, and 24 h. The

experiment was performed more than three times, and the rate of migration was calculated.

Measurement of transepithelial electric resistance. Myo1c knockdown and control human podocytes were grown in 12-well cell culture Transwell filters (0.4-μm pore; Corning, New York, NY) until they became completely confluent. Transepithelial electric resistance (TER) was measured by using an epithelial volt-ohmmeter (model EVOM; World Precision Instruments) at 3 days postconfluence (considered day 0). The measurements were taken every 24 h for the next 4 days. The TER of a control well without cells was also measured in parallel as a control. To determine the presence of tight junctions in these podocytes, a control experiment was performed where TER was measured in normal podocyte cells, these wells were then treated with Ca^{2+}/Mg^{2+}-depleted medium for a period of 10 min, and the TER was measured again. Absolute TER values were determined by subtracting the TER of blank filters with medium from values for all samples and are presented as the measured resistance in ohms divided by the surface area (1.12 cm^2) of the Transwell filter.

Measurement of albumin flux. The transepithelial permeability of control and Myo1c knockdown cells for BSA was assessed by measuring the passage of Texas Red-labeled BSA across the podocyte monolayer. At 3 days postconfluence, cells were washed with 1× PBS, and the medium in wells (lower chamber) and inserts (upper chamber) was replaced with serum-free medium. Texas Red-labeled BSA at a final concentration of 50 μg/ml was added to the wells of the Transwell plate. Aliquots were removed from the insert at regular intervals to measure the fluorescence with excitation at 590 nm and emission at 625 nm. A standard curve derived from the measurement of serial dilutions of Texas Red-labeled BSA was used to calculate the amount of BSA moved from the well to the insert. A Transwell without cells and cells treated with Ca^{2+}/Mg^{2+}-depleted medium were used as controls.

RESULTS

We previously demonstrated that glomerular injury induces dynamic changes in the Neph1 complex, thereby inducing the intracellular movement of Neph1, which may involve intracellular transport-based mechanisms (47). This prompted us to utilize a proteomic-based approach to determine if motor proteins are components of the Neph1 complex.

Identification of Myo1c as a Neph1-interacting protein. To enrich the recovery of Neph1 complexes, cell lysates from a human podocyte cell line overexpressing wild-type (wt) Neph1 were used, and the Neph1 complexes were captured on a Neph1 antibody affinity matrix. The identification of unique bands from SDS-PAGE gels by mass spectrometry showed the presence of Myo1c (100 kDa) in the Neph1 complex (Fig. 1A). Additionally, ZO-1 (a known interactor for Neph1) and Neph1 were also identified in the screen, confirming the validity of our approach. Note that these proteins were selectively isolated from the Neph1 affinity column and were absent from the control antibody column (Fig. 1B). Western blotting of the eluate from the Neph1 affinity column further confirmed the presence of Myo1c in the Neph1 complex (Fig. 1C).

Various myosin I family members are expressed in cultured podocytes. To analyze the expressions of various myosin I family members in podocytes, mRNA isolated from cultured human podocytes was subjected to RT-PCR analysis. Myo1b, Myo1c, Myo1d, and Myo1e mRNAs were expressed in both differentiated and undifferentiated (Fig. 1D) cultured podocytes. To further analyze the expression of myosin I proteins in glomeruli and podocytes, rat glomerular lysates and cell lysates from cultured podocytes were probed with antibodies specific to Myo1c, Myo1b, Myo1d, and Myo1e and analyzed by Western blotting. The Myo1c, Myo1b, Myo1d, and Myo1e proteins were present in the glomerular lysate, but only the Myo1c, Myo1b, and Myo1e proteins were detected in the podocyte cell lysate (Fig. 1E). Although the RT-PCR results suggest that the Myo1d transcript is present in podocytes, the absence of the Myo1d protein in the cell lysate indicates either a posttranslational modification or rapid degradation of Myo1d to levels beyond detection by Western blotting. During the preparation of the manuscript, a report analyzing the slit diaphragm proteome was published, which described the presence of multiple myosins, including Myo1b, Myo1c, Myo1d, and Myo1e (38). In addition to myosin I proteins, MyoV and MyoVI are also present in human podocytes (Fig. 1D).

Neph1 interacts with Myo1c under *in vivo* and *in vitro* conditions. To further determine the specificity of Neph1 and Myo1c interactions, Neph1 was immunoprecipitated from podocyte cell lysates, and the immunoprecipitated complex was analyzed for the presence of various myosin I proteins. Interestingly, only Myo1c interacted with Neph1 (Fig. 2A). To extend these observations, a similar immunoprecipitation experiment was performed with rat glomerular lysate, which further confirmed the interaction between Neph1 and Myo1c (Fig. 2B). In a reciprocal experiment, the immunoprecipitation of Myo1c from podocyte cell lysates further supported Neph1 binding to the motor protein Myo1c (Fig. 2C). Further data supporting an interaction between Myo1c and Neph1 were obtained by overexpressing GFP-Myo1c and Flag-Neph1 in COS-7 cells, where Myo1c immunoprecipitated with Neph1 (Fig. 2D). To further establish a direct interaction between Neph1 and Myo1c, a pulldown experiment was performed, where the recombinant His-tagged or GST-tagged cytoplasmic domain of Neph1 was mixed with recombinantly purified full-length Myo1c (Fig. 2E). Data from the analysis of the Neph1 pulldown complex are consistent with Neph1 directly interacting with Myo1c (Fig. 2E). Overall, these results support that Neph1 interacts with Myo1c under *in vivo* and *in vitro* conditions.

Myo1c colocalizes with Neph1 in glomeruli and cultured podocytes. Since the location of Myo1c in the glomerulus was not characterized previously, we examined the distribution of Myo1c within glomeruli, using both microscopic and biochemical methods. Using immunofluorescence, we first analyzed the presence of Myo1c in rat glomeruli, where Myo1c immunoreactivity was indeed detected (Fig. 3A). To determine whether the immunoreactivity was present in podocytes, paraffin-embedded adult rat kidney sections were double labeled with a rabbit anti-Neph1 antibody (Fig. 3A). Merged images demonstrated Myo1c expression in podocytes, where it partially colocalizes with Neph1. Further preincubation of the Myo1c antibody with the purified Myo1c protein completely blocked the Myo1c staining of the glomerulus, confirming the specificity of this antibody (Fig. 3B). Figure 3C and D show immunoelectron microscopy of rat kidney sections using postembedding colloidal gold immunolabeling of rat kidney sections. The presence of gold particles in the foot processes at or close to the slit diaphragm (Fig. 3B and D) supports a localization pattern similar to that of Neph1 (2). In addition, gold particles were also located inside the podocyte cell body (Fig. 3D), consistent with a widespread distribution of Myo1c in podocytes. Neph1 associates in part with a Triton X-100-insoluble membrane fraction obtained from isolated glomeruli (2). To evaluate if Myo1c is a component of the Neph1 signaling complex and, hence, is present in the same membrane fraction, rat glomeruli were isolated, lysed, and fractionated as described previously by using Optiprep (2). Each fraction was analyzed by immunoblotting for caveolin (lipid raft marker), transferrin receptor

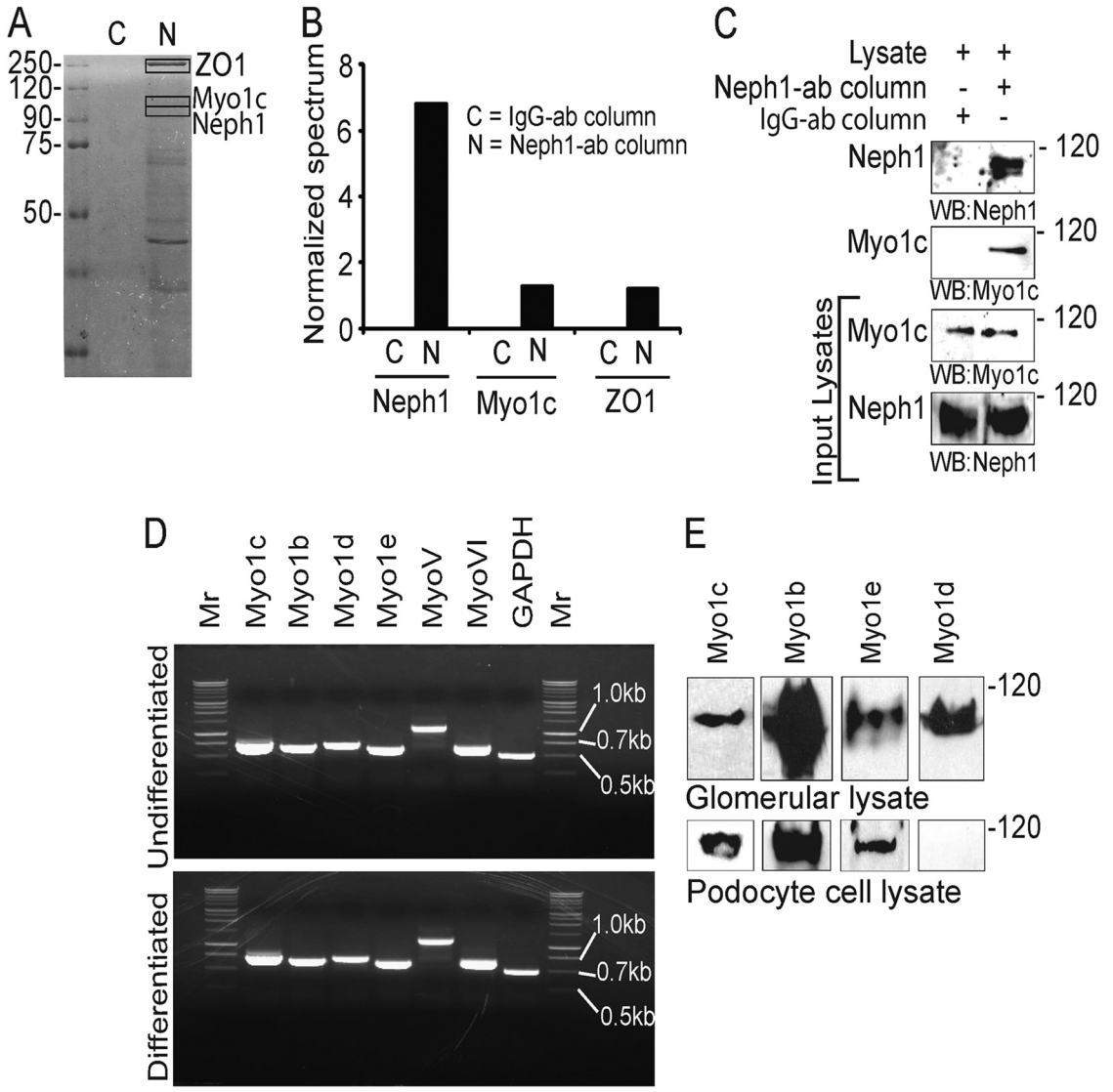

FIG. 1. Identification of Myo1c as a Neph1 binding protein. (A) Eluates from Neph1 affinity and control columns were separated on SDS-PAGE gels and subjected to mass spectrometry. Protein bands containing ZO-1, Neph1, and Myo1c are highlighted. (B) Normalized spectrum values derived by using Scaffold software (Proteome Software, Inc., Portland, OR). (C) The same eluate was probed with Neph1 and Myo1c antibodies to confirm the results from the mass spectrometry analysis. Various myosin I proteins are expressed in human podocytes. (D) RT-PCR of differentiated and undifferentiated cultured human podocytes with the indicated primers detects various myosin family members. Mr, marker. (E) Cultured human podocytes and rat glomerular lysates were Western blotted (WB) with various class I myosin antibodies.

(non-lipid raft marker), Neph1, Myo1c, nephrin, podocin, and ZO-1 (Fig. 3E). Similarly to other slit diaphragm proteins, including nephrin, Neph1, and podocin, Myo1c also localized in the detergent-resistant lipid raft fractions (fractions 3 and 4) (Fig. 3E). In a similar fashion, a fractionation analysis of podocyte cell lysates further confirmed the colocalization of Myo1c with Neph1 in the lipid raft fractions (Fig. 3F). Overall, these results are consistent with an interaction between Myo1c and Neph1.

The principal model system that has been widely used to study the basic function of slit diaphragm proteins is the *in vitro* cell culture model. We reported previously that Neph1 is located at the podocyte cell membrane and enriched at the cell periphery, where it colocalizes with ZO-1 (47). To determine the location of Myo1c in this system, cultured human podocyte cells were analyzed by immunofluorescence microscopy. As reported previously, in addition to staining in the perinuclear region, Neph1 was enriched at the podocyte cell membrane (Fig. 4A). The enlarged-image panel on the right of Fig. 4A indicates the colocalization of Neph1 and Myo1c at the cell membrane. Note that unlike Neph1, Myo1c is widely distributed but enriched at the plasma membrane and cell junctions (Fig. 4A), where maximum colocalization with Neph1 was observed, with a Pearson's correlation coefficient of 0.4 (Fig. 4A and C). In addition, Myo1c and Neph1 stainings were also observed in the cellular processes extending from one cell to the other (Fig. 4B). Together, these results support the existence of a complex of Neph1 and Myo1c that is enriched at the podocyte cell membrane and cell junction.

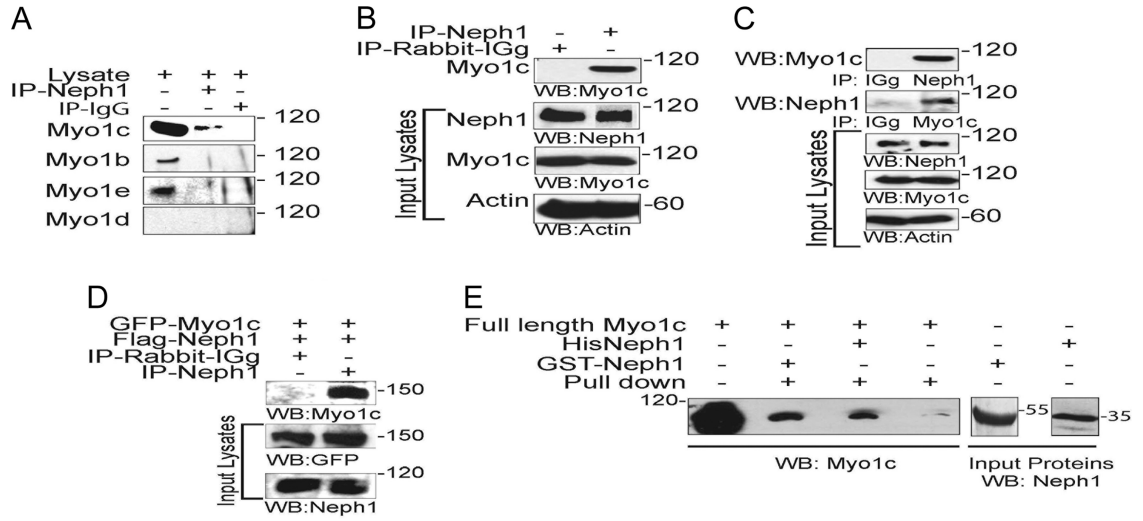

FIG. 2. Neph1 interacts with Myo1c under *in vivo* and *in vitro* conditions. (A) Immunoprecipitation was performed with podocyte cell lysates using Neph1 antibody, and Western blotting was performed with antibodies specific to Myo1c, Myo1b, Myo1e, and Myo1d to determine their interactions with Neph1. (B) Neph1 was immunoprecipitated (IP) from rat glomerular lysates and immunoblotted with Myo1c antibody to confirm the interaction between Neph1 and Myo1c. (C) Reciprocal immunoprecipitation in cultured human podocytes using Myo1c antibody and Western blotting with Neph1 confirms the Neph1 and Myo1c interaction. (D) Plasmids encoding full-length GFP-Myo1c and Flag-Neph1 were transfected into COS-7 cells. Neph1 was immunoprecipitated from the cell lysate, and the immune complex was analyzed for Myo1c binding using Myo1c antibody. (E) The recombinant purified cytoplasmic domain of Neph1 as a GST or His fusion protein was mixed with purified full-length His-Myo1c expressed in baculovirus. Pulldown with either GST beads or Neph1 antibody and Western blotting with Myo1c antibody show binding between Neph1 and Myo1c.

Neph1 localization at the membrane is actin dependent. If Myo1c is serving as a motor that targets Neph1 to the plasma membrane, actin will serve as the track. Consequently, actin but not microtubule disruption would be expected to alter Neph1's distribution. To test this hypothesis, podocytes were treated with actin and the microtubule-depolymerizing agents latrunculin B and nocodazole and analyzed by immunofluorescence. The results presented in Fig. 5A document that the treatment of cultured podocytes with latrunculin B significantly altered the location of Neph1 and Myo1c from the plasma membrane to the perinuclear region, where they still appeared to be colocalized. In contrast, treatment with nocodazole had a minimal effect on the distribution of Neph1 and Myo1c, supporting the hypothesis that an intact actin cytoskeleton is required for the proper location of Neph1 in podocytes (Fig. 5A and B). The staining of the plasma membrane with the membrane marker WGA further demonstrated that unlike nocodazole, the loss of the actin cytoskeleton in latrunculin B-treated cells also altered the plasma membrane (Fig. 5B). Glomerular injury models that disrupt the actin cytoskeleton network also induce the loss of podocyte function, with proteinuria and renal failure (22, 25, 27). We previously demonstrated that glomerular injury induced by ischemia results in the loss of Neph1 interactions that are critical for maintaining the integrity of the slit diaphragm structure and function (10, 19, 24, 47). To determine if renal injury induces similar dynamic changes in Neph1 and Myo1c complexes, Neph1 and Myo1c binding was analyzed in a rat ischemia model and a PAN injury model with cultured podocytes (47). As shown in Fig. 5C, the interaction of Neph1 and Myo1c was dramatically reduced after 45 min of ischemia. Importantly, this interaction was restored after 4 h of reperfusion (Fig. 5C). Similarly, in the PAN-induced podocyte injury model, the treatment of podocyte cells with PAN resulted in a significant decrease in the interaction between Neph1 and Myo1c, which was restored upon recovery from PAN (Fig. 5D). Together, these results provide evidence of a dynamic interaction between Neph1 and Myo1c that is significantly altered by glomerular injury but, importantly, retains its capacity to recover following reperfusion. These results further suggest that glomerular injuries that alter the podocyte actin cytoskeleton also regulate the interaction between Neph1 and Myo1c.

Localization of Neph1 to the podocyte cell membrane is altered in the presence of mutant Myo1c. Based on the above-described results we hypothesized that Myo1c is an integral component of the Neph1 complex and uses its motor function to regulate the organization of the Neph1 complex. To address this hypothesis, we used a recognized and proven approach to study the trafficking function of Myo1c (5, 30, 50). In this assay, cultured human podocytes transfected with either wild-type GFP-Myo1c or mutant GFP-Myo1c (Myo1c 690-1028), lacking both ATP and actin binding domains (dominant negative), were analyzed by immunofluorescence. Untransfected cells and cells transfected with wt Myo1c showed Neph1 at the cell membrane, cell periphery, and fine processes that extend from the cells (Fig. 6A). In striking contrast, Neph1 was not present at the cell periphery or at the cell membrane (Fig. 6A, right) in cells transfected with mutant Myo1c. A quantitative assessment of these images suggests a significant reduction (>60%) in Neph1 localization at the cell periphery in cells expressing mutant Myo1c (Fig. 6B). Unlike Neph1, the transfection of mutant GFP-Myo1c did not alter the membrane localization of ZO-1 (Fig. 6C), indicating that Myo1c specifi-

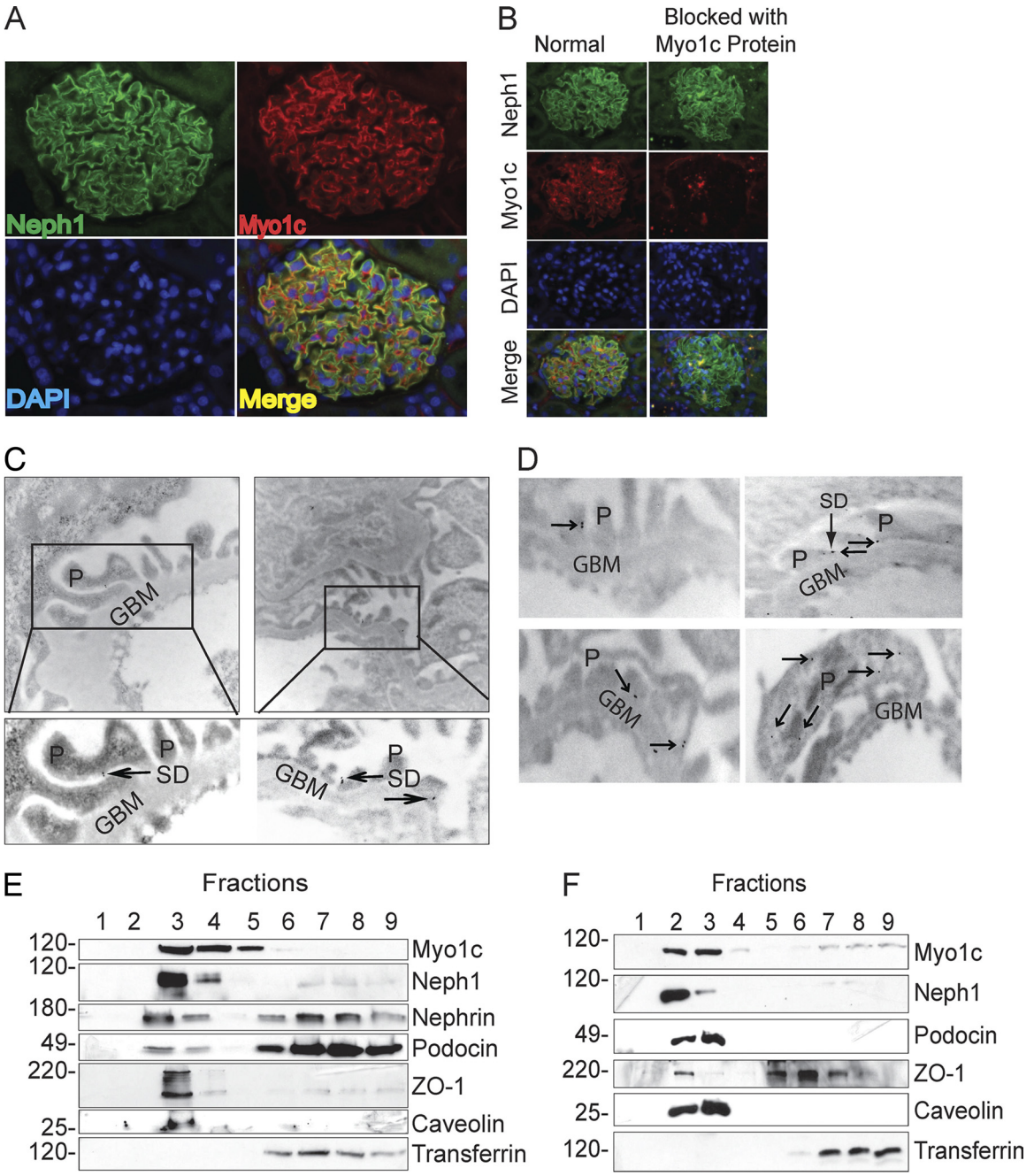

FIG. 3. Myo1c is a podocyte protein and colocalizes with Neph1. (A) Kidney sections from PFA-perfused rats were immunostained with Myo1c and Neph1 antibodies to determine the colocalization of Myo1c (red) with Neph1 (green) in glomeruli. (B) To determine the specificity of the Myo1c antibody, it was preincubated with the Myo1c protein prior to staining. Nuclear staining was performed with DAPI (blue). (C and D) Immunogold electron micrographs of kidney sections stained with Myo1c antibody show Myo1c localization adjacent to the slit diaphragm (arrows). P, podocytes; GBM, glomerular basement membrane; SD, slit diaphragm. (E and F) Lysate obtained from mouse glomeruli (E) or cultured human podocytes (F) was subjected to flotation gradient centrifugation using Optiprep. Fractions were analyzed by immunoblotting with the indicated antibodies. Western blotting with caveolin antibody identified the lipid raft fraction (fraction 3 at the interface between the 5 and 30% Optiprep densities).

cally alters the localization of Neph1 at the podocyte cell membrane.

Knockdown of Myo1c inhibits Neph1 membrane localization. Since the introduction of a dominant negative Myo1c mutant into podocytes affected Neph1's membrane localization, we next hypothesized that a deletion of Myo1c would cause similar or additional changes. To accomplish this, five different plasmid constructs encoding Myo1c-specific small hairpin RNAs (shRNAs) were transfected into cultured human podocytes. In an effort to induce long-term gene silencing,

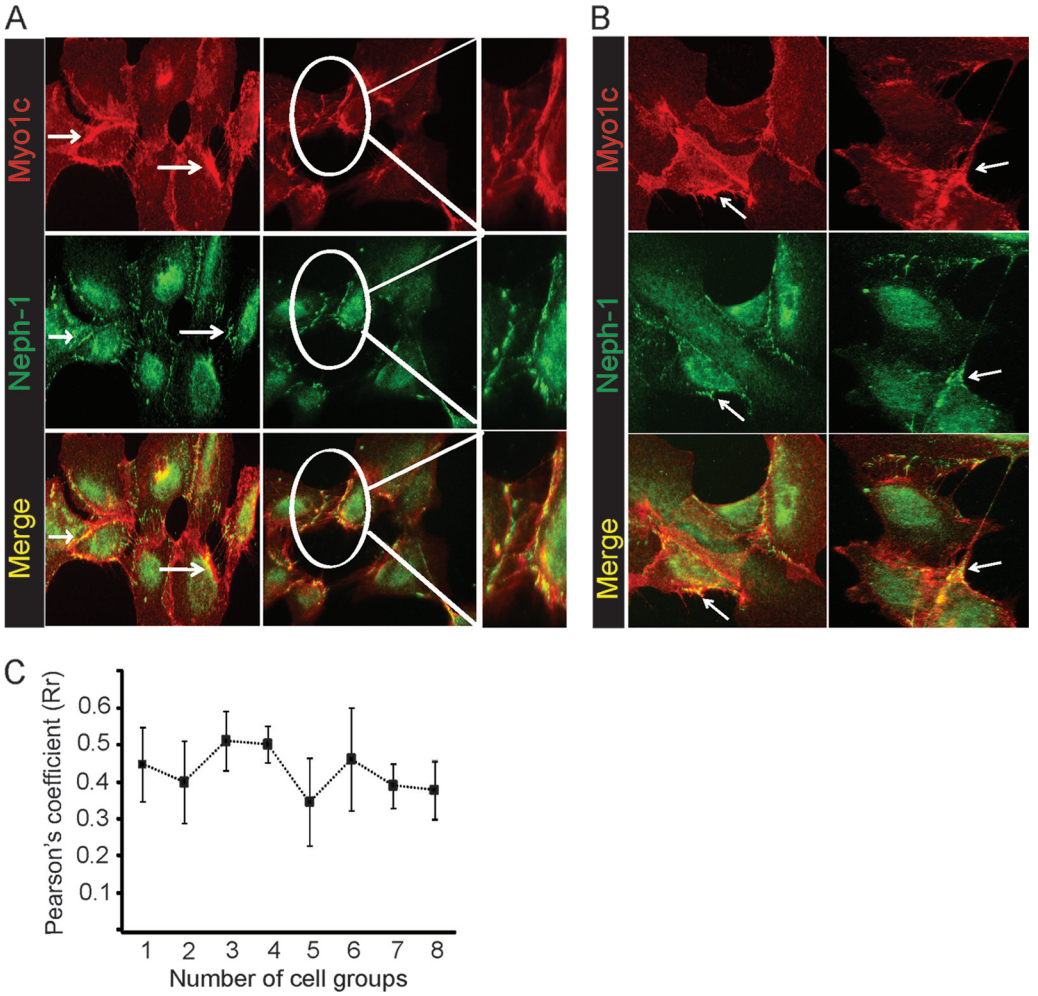

FIG. 4. Myo1c and Neph1 colocalize in cultured human podocytes. (A and B) Cultured podocytes grown on coverslips were fixed with 4% PFA and immunolabeled with Myo1c (red) and Neph1 (green) antibodies. As noted previously, Neph1 is concentrated at the cell membrane, while Myo1c is widely distributed in the cytoplasm and enriched at the cell membrane. The red-green overlay (yellow) shows Myo1c and Neph1 colocalization close to the cell membrane, in cell processes or lamellipodia, and also at cell-cell contacts in adjacent enlarged images. Representative images from five different experiments are shown, the junction region from one set of images is enlarged, and Neph1 and Myo1c colocalization is highlighted. (C) The Pearson's correlation coefficient (*Rr*) at the cell boundary of podocytes was calculated by using Image J software and shows a partial colocalization of Myo1c with Neph1, with an *Rr* of ~0.4. Eight different cell groups ($n = 8$ cells) were included from five different experiments for quantitation.

transfected cells were selected for the stable expression of Myo1c shRNA. Next, the level of Myo1c protein knockdown was quantified by using Western blotting. A maximum knockdown of over 80% was achieved for Myo1c with one of the five shRNAs (Fig. 7A and C), which was used for all subsequent experiments. The specificity of the Myo1c shRNA was further determined by estimating the protein levels of Neph1 and Myo1e that remained unaltered in Myo1c knockdown cells (Fig. 7I). The knockdown of Myo1c was further analyzed by immunofluorescence using a Myo1c antibody, confirming the reduction in Myo1c staining (Fig. 7B). Next, we evaluated the impact of the Myo1c deletion on the cell distribution of Neph1 by immunofluorescence. A significant reduction in the level of Neph1 at the cell membrane and cell junctions was observed (Fig. 7B). Representative images from five different experiments are shown to demonstrate the distribution of Neph1 in the podocyte cells (Fig. 7B). In addition, fractionation analysis of Myo1c knockdown cells further showed a reduction in the level of Neph1 in the membrane fraction (Fig. 7J). The quantitation of cell peripheral fluorescences for both Myo1c and Neph1 from 3 independent experiments (n of 15 cells under each condition) confirmed a significant reduction in levels of both proteins at the cell membrane (Fig. 7D and E). To further confirm the loss of Neph1 from the membrane of podocytes, Myo1c knockdown and control podocyte cells were stained with Neph1 antibody directed toward the extracellular domain of Neph1. As shown in Fig. 7F, the staining of surface Neph1 in Myo1c knockdown cells was significantly reduced. A quantitative analysis of these cells suggests a >80% reduction in antibody intensity at the membrane of Myo1c knockdown cells (Fig. 7G). As expected, the knockdown of Myo1c did not affect ZO-1 localization at the membrane (Fig. 7H). To extend these observations, we hypothesized that the introduction of Myo1c into the knockdown cells would restore Neph1 to the podocyte

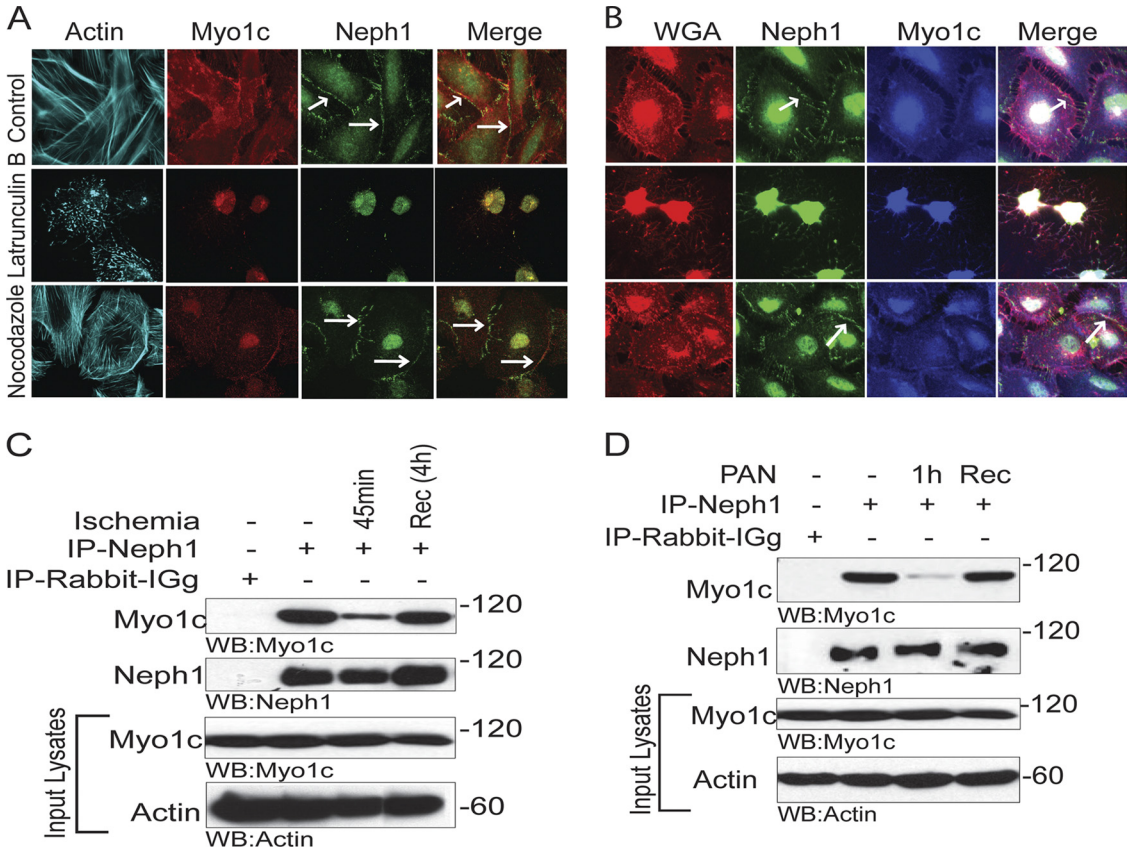

FIG. 5. The interaction of Neph1 and Myo1c is actin dependent. (A and B) Cultured podocytes grown on coverslips were treated with either latrunculin B (5 mM), nocodazole (30 μM), or growth medium for 1 h. Cells were then washed and processed for immunostaining with phalloidin (Alexa 488), Myo1c (Alexa 568/350), and Neph1 (Alexa 647/488) antibodies and with the membrane marker WGA (Alexa 594) (B). While latrunculin B induced the mislocalization of Myo1c and Neph1, treatment with nocodazole or normal medium had little effect. Renal injury induces the dissociation of the complex of Neph1 and Myo1c. (C) Male Sprague-Dawley rats were subjected to bilateral ischemia for 45 min with a reperfusion/recovery (Rec) time of 4 h. Isolated glomeruli were lysed in RIPA buffer. Neph1 was immunoprecipitated from glomerular lysates of control, ischemic, and recovered mice and Western blotted with Myo1c and Neph1 antibodies. (D) Podocyte cell lysates obtained from cells treated with PAN and from PAN treatment followed by recovery were subjected to Neph1 immunoprecipitation and Western blotted with Myo1c and Neph1 antibodies. Equivalent amounts of Neph1 and Myo1c were also examined, and actin was used as a loading control. These experiments were repeated three times, with identical results.

cell periphery. To test this hypothesis, Myo1c knockdown cells were transfected with mouse GFP-Myo1c cDNA (which is resistant to human Myo1c shRNA) or control cDNA (empty vector), and the cells were immunostained for Neph1. As shown in Fig. 8A, Neph1 returned to the cell periphery in cells expressing wild-type GFP-Myo1c and not the control vector. A quantitative analysis of these images further confirmed the rescue of Neph1 at the cell periphery in mouse GFP-Myo1c-expressing cells (Fig. 8B). Note that adjacent cells (untransfected) displayed very little Neph1 at the periphery (Fig. 8A, right).

Clustered Neph1 is not recruited to the podocyte membrane in Myo1c knockdown cells. To further confirm the role of Myo1c in the trafficking of Neph1 to the podocyte cell membrane and its activation, we studied the effect of the Myo1c knockdown on the localization of chimeric Neph1, where the extracellular and transmembrane domains of Neph1 were replaced with a CD16 antibody binding domain and a CD7 transmembrane domain (10, 45). In this model system (10), the addition of CD16 antibody followed by secondary anti-mouse IgG antibody in live cells clusters chimeric Neph1 at the cell surface. As noted previously, the "clustering" of CD16-Neph1 on the plasma membrane was readily visualized by epifluorescence microscopy (Fig. 9A and B) and confocal microscopy (Fig. 9C) of control cells. In contrast, CD16-Neph1 clustering at the cell membrane was significantly reduced in Myo1c knockdown cells (Fig. 9). Quantitation of the CD16 pixel intensity suggested a >90% reduction in the level of Neph1 at the membrane of Myo1c knockdown cells (Fig. 9B). Collectively, these results provide strong evidence that the Myo1c motor-based mechanism is required for the translocation of Neph1 to its functional site at the podocyte cell membrane.

Myo1c binds nephrin and mediates the membrane localization of nephrin. Neph1 and nephrin share similar structural and functional properties and are engaged at extracellular and intracellular levels to maintain the integrity of the slit diaphragm and, therefore, podocyte function (24, 44). Since Myo1c had a profound effect on Neph1 localization, we hypothesized that Myo1c also plays a role in mediating the intracellular movement of nephrin. To test this, we first analyzed

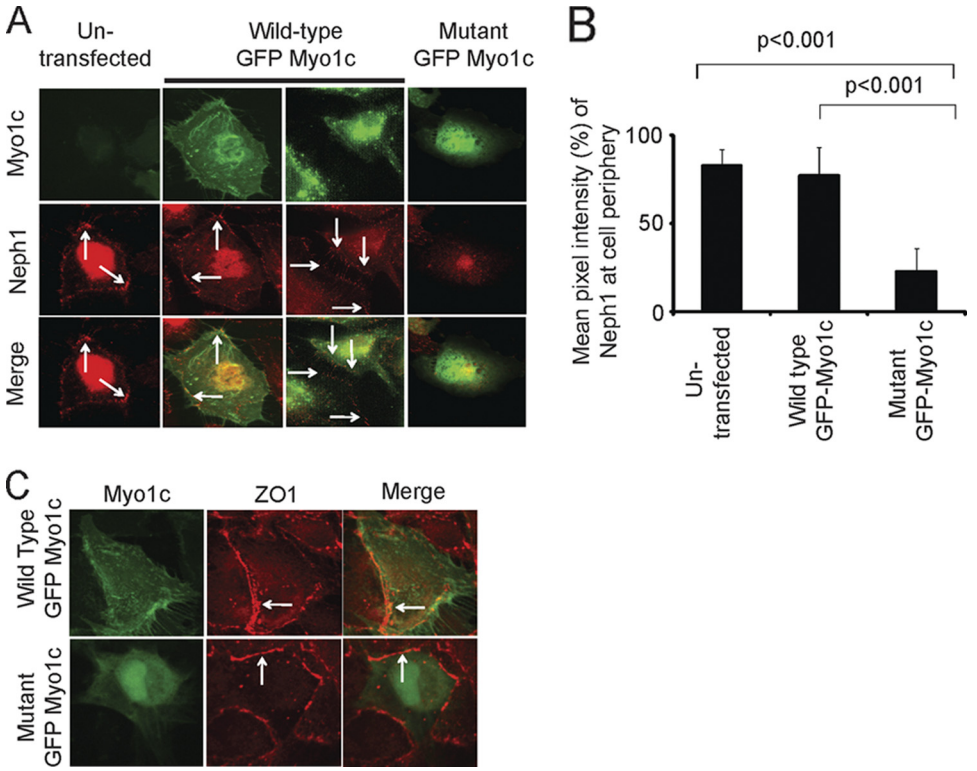

FIG. 6. Neph1 localization at the podocyte cell membrane is altered in the presence of dominant negative Myo1c. (A and C) Human podocytes transfected with wt GFP-Myo1c or dominant mutant GFP-Myo1c (without ATP and actin binding domains) were analyzed by immunofluorescence with Neph1 (A) or ZO-1 (C) antibodies. Note the presence of Neph1 and ZO-1 at the cell membrane (arrows) in untransfected cells and cells transfected with wt Myo1c. In contrast, cells transfected with mutant GFP-Myo1c showed a significant reduction in the amount of Neph1 but not of ZO-1 at the cell membrane. (B) Quantitative analysis of transfected and untransfected cells was performed ($n = 10$ cells), and the bar diagram shows the mean pixel intensities of Neph1 at the cell periphery.

the interaction between nephrin and Myo1c by immunoprecipitating nephrin from mouse glomerular lysates and Western blotting for Myo1c. As shown in Fig. 10A, Myo1c immunoprecipitated with nephrin. To further establish a direct interaction, a GST pulldown experiment was performed, where the purified recombinant GST-tagged cytoplasmic domain of nephrin was incubated with purified recombinant full-length Myo1c. Analysis of the GST pulldown indicated a direct interaction between nephrin and Myo1c (Fig. 10B). Overall, these results support the hypothesis that nephrin interacts with Myo1c under *in vivo* and *in vitro* conditions. We next examined if, similarly to Neph1, the localization of nephrin is also affected in Myo1c-deficient podocytes. Since cultured human podocytes express very small amounts of the nephrin protein, we analyzed the localization of nephrin in podocytes using the CD16 model system (45). As demonstrated previously, the "clustering" of CD16-nephrin at the plasma membrane in control cells was readily visualized by confocal microscopy (Fig. 10C). In contrast, CD16-nephrin clustering was significantly reduced in Myo1c knockdown cells (Fig. 10C and D). Quantitation of CD16 pixel intensity in Myo1c knockdown cells suggested a >70% reduction in the level of nephrin at the membrane (Fig. 10D). In conclusion, these results indicate that in a fashion similar to that of Neph1, Myo1c also binds nephrin and affects its localization at the cell membrane.

Myo1c knockdown podocytes exhibit decreased cell migration, reduced TER, and increased permeability for BSA. Since Myo1c inhibits the membrane localization of Neph1 and nephrin and it has been implicated as having a role in actin dynamics, organelle movements, and membrane ruffling in various cell types (3, 13), we hypothesized that the loss of Myo1c would adversely affect podocyte migration and function. To investigate this, we tested the integrity and functionality of Myo1c knockdown podocytes by determining their rate of migration and ability to form tight junctions. Therefore, a wound assay was performed to determine the rates of cell migration in Myo1c knockdown and control podocytes. As shown in Fig. 11A, complete wound closure was observed for control cells after 24 h, but Myo1c knockdown cells covered only 70% of the control area. This migration defect was consistently observed in three independent experiments (Fig. 11B). Importantly, this phenotype was rescued with the overexpression of full-length GFP-Myo1c in Myo1c knockdown podocytes (Fig. 11A and B). Quantitative analysis further suggested a significant reduction in the mean rate of migration of knockdown cells compared to that of the control cells (Fig. 11B). We next examined whether the Myo1c knockdown affects the function of the podocyte monolayer as a tight-junction barrier. To first analyze the tight-junction dynamics, control and Myo1c knockdown podocyte cells were grown to confluence and then subjected to TER

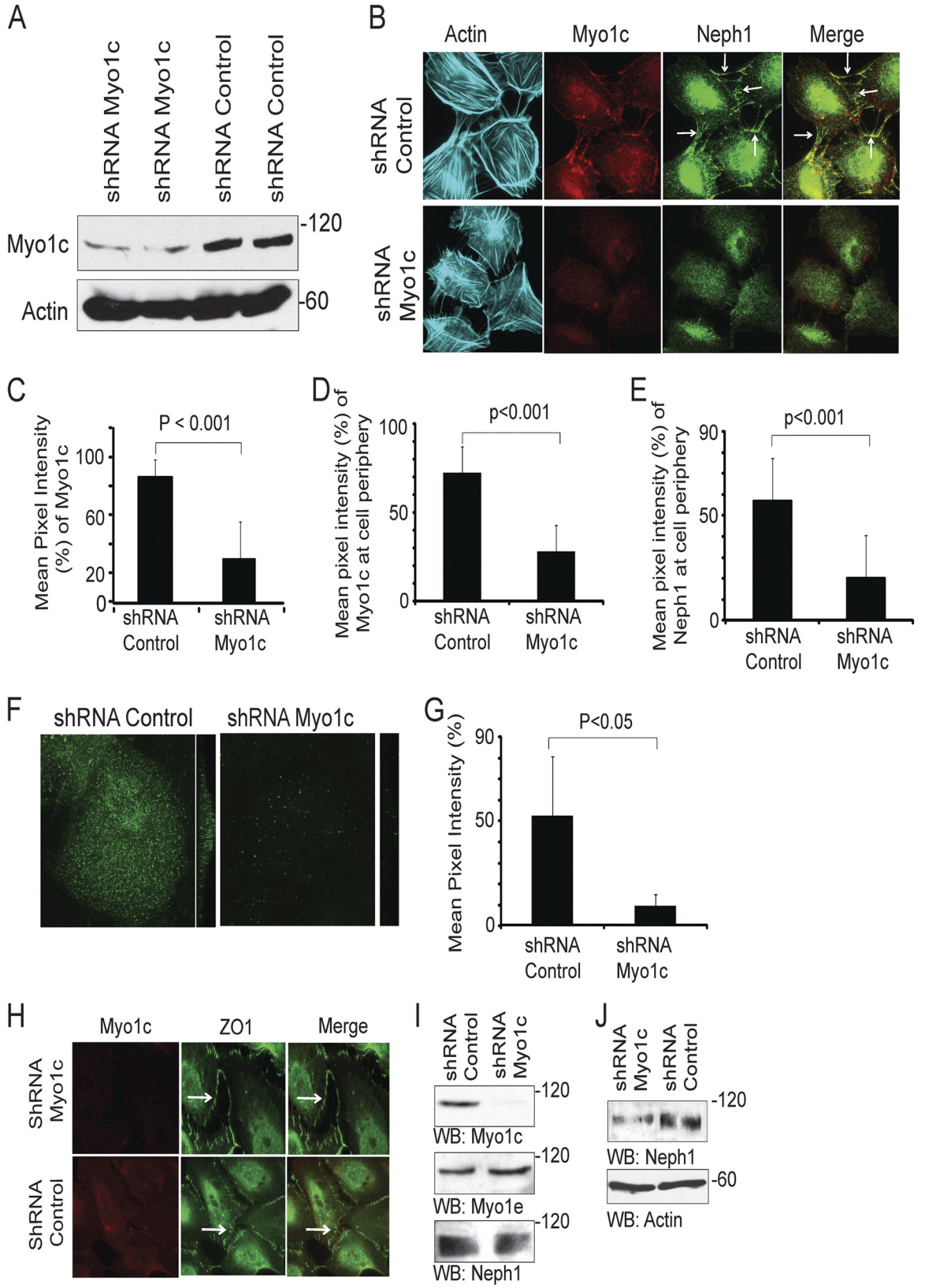

FIG. 7. shRNA-mediated Myo1c knockdown inhibits Neph1 membrane localization. (A) Myo1c knockdown was induced by the transfection of a plasmid encoding Myo1c shRNA in cultured human podocytes. Stable transfectants were selected, and the extent of the Myo1c protein knockdown was assessed by Western blotting. (B) Control and knockdown cells were analyzed by immunofluorescence using Myo1c (Alexa 568) and Neph1 (Alexa 488) antibodies and phalloidin (Alexa 488). (C) Quantitation of Myo1c knockdown from five different experiments is

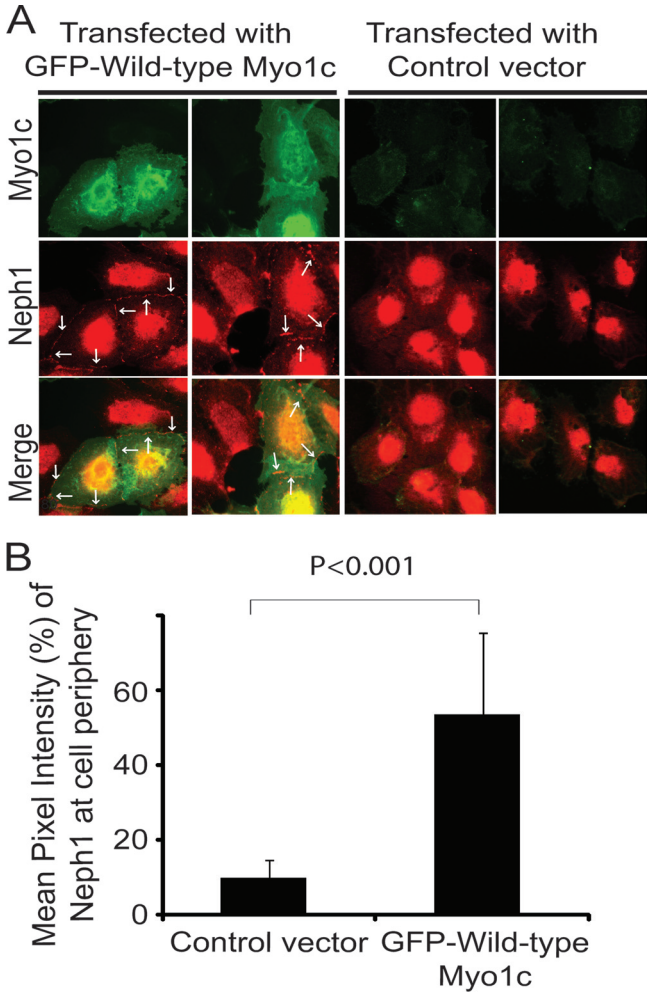

FIG. 8. Transfection of mouse GFP-Myo1c rescues Neph1 membrane localization in Myo1c knockdown cells. (A) Myo1c knockdown cells were transfected with either mouse GFP–full-length Myo1c or a control vector and stained with Neph1 antibody (red). Neph1 localizes at the cell periphery only in GFP-Myo1c-transfected cells (arrows). (B) Quantitative analysis was performed on data from three independent experiments ($n = 10$ cells) to calculate the mean pixel intensity of Neph1 at the cell periphery in transfected cells.

measurements, as shown in Fig. 11C. The electrical resistance was measured over a period of 5 days postconfluency, and the reduced TER in Myo1c knockdown cells suggests a decrease in their ability to form tight junctions (Fig. 11C). Next, albumin filtration across the monolayer of cultured control and Myo1c knockdown cells was assessed by a paracellular albumin flux assay using Texas Red-labeled albumin. Increased albumin flux was observed for Myo1c knockdown podocytes compared to control cells (Fig. 11D). To further determine if the loss of Neph1 also induced similar defects in podocytes, we performed a parallel Neph1 knockdown experiment using Neph1-specific shRNA (Fig. 11E and F). Similarly to Myo1c knockdown cells, the depletion of Neph1 in podocytes also resulted in reduced TER and increased permeability for BSA (Fig. 11G and H). Collectively, these results indicate that the loss of Myo1c is consistent with the loss of Neph1 in podocytes and reduces the ability of podocytes to form tight junctions, with a loss of permeability for proteins.

DISCUSSION

Podocyte proteins localized at the slit diaphragm have critical functions of maintaining the podocyte structure and provide a platform for the assembly of signaling complexes. Studies of many glomerular diseases in humans and mice have documented changes in podocyte protein dynamics, including a loss of interactions between slit diaphragm proteins and their translocation to different subcellular locations (8, 34, 49). Using animal and cell culture models, we previously demonstrated similar changes in Neph1 protein dynamics in response to glomerular injury (47). However, the molecular and cellular mechanisms associated with these changes that contribute to the maintenance of the slit diaphragm remain largely unknown. Our identification of the motor protein Myo1c as a novel component of the slit diaphragm and its ability to associate with Neph1 and nephrin suggests that a molecular motor-based mechanism organizes the slit diaphragm complex at the podocyte cell membrane.

Motor proteins from the myosin I family, including Myo1c, are enriched in membrane structures and localized to filopodia, lamellipodia, ruffles, and the leading edges of migrating cells, in addition to a cytoplasmic punctate pattern (3, 46). We observed a similar pattern for Myo1c in cultured podocytes, with partial Neph1 colocalization at the cell periphery. In addition, unlike Neph1, Myo1c also had a cytoplasmic distribution, as described previously for multiple cell types (46). Additional evidence for the Myo1c and Neph1 association comes from the colocalization observed for rat glomerular sections and from analyses of lipid raft fractions from mouse glomeruli and podocyte cells that showed a significant overlap of Neph1 and Myo1c in the same subcellular compartments. Although podocytes in cell culture do not form *in vivo* like foot processes, they do form dynamic structures such as lamellipodia, membrane ruffles, and long filopodium-like structures that can extend from one cell to the other. All these structures are

represented as the mean pixel intensity of Myo1c. (D and E) Mean pixel intensity analysis of Myo1c and Neph1 at the podocyte cell membrane from five different experiments (15 cells each) was performed and shows a significant reduction in the amount of Neph1 at the cell membrane compared to control shRNA ($P < 0.001$). (F) Surface Neph1 was labeled in Myo1c knockdown and control cells with Neph1 extracellular antibody under unpermeabilized conditions. Immunofluorescence analysis was performed by using confocal imaging. (G) Quantitative analysis of single-plane images ($n = 10$ cells) shows a significant decrease in the mean pixel intensity of surface Neph1 labeling in Myo1c knockdown cells compared to control cells. (H) Immunofluorescence analysis of Myo1c knockdown cells with ZO-1 antibody shows that ZO-1 localization remains unchanged compared to control shRNA. (I) Lysates from control and Myo1c knockdown cells were Western blotted with Myo1c, Neph1, and Myo1e antibodies and show that Myo1c knockdown does not alter Neph1 and Myo1e protein levels. (J) Myo1c and control knockdown cells were fractionated to isolate the membrane fractions, which were analyzed by Western blotting using Neph1 antibody.

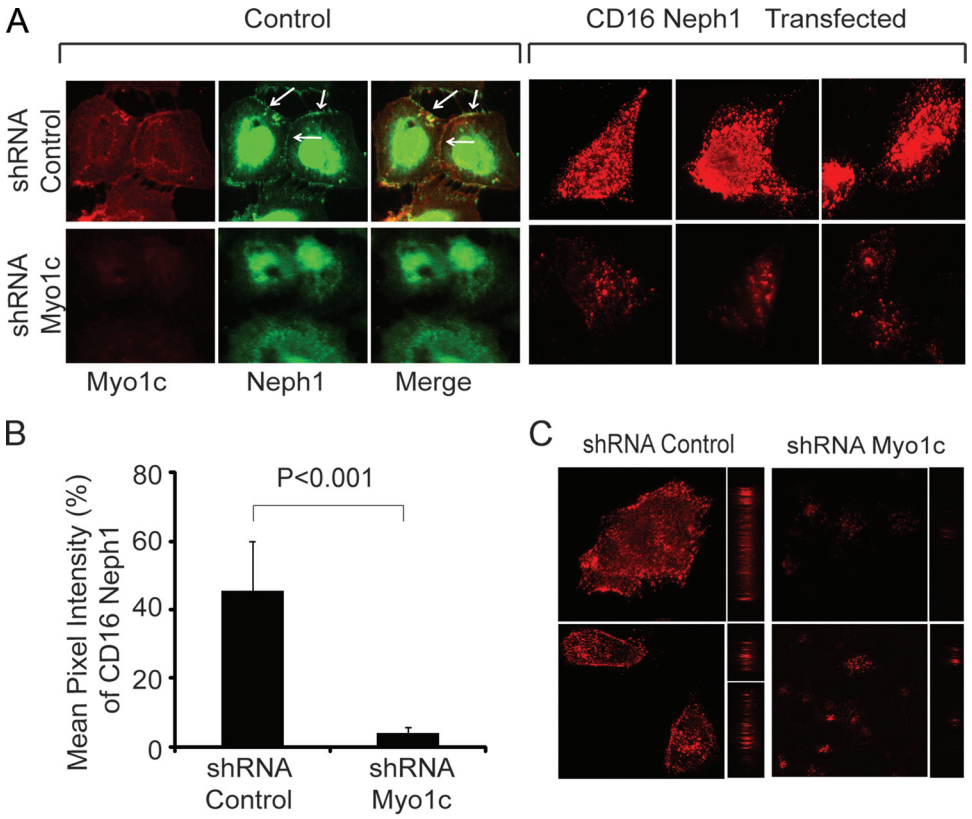

FIG. 9. Clustering of Neph1 at the podocyte membrane is inhibited in Myo1c-deleted cells. (A) A plasmid encoding the CD16-Neph1 cytoplasmic domain was transfected into Myo1c knockdown and control cells. (Right) Live cells were processed for clustering with CD16 antibody and analyzed by immunofluorescence. (Left) A parallel set of untransfected cells (control) was immunostained with Neph1 and Myo1c antibodies to determine the extent of the Myo1c knockdown. Representative images from three independent experiments are shown. (C) The same cells were also analyzed by confocal microscopy. (B) Quantitative analysis of transfected cells (n = 10 cells) shows a significant decrease in the mean pixel intensity of CD16-Neph1 in Myo1c knockdown cells compared to control cells.

sites of active actin dynamics involving multiple cytoskeletal elements that together help regulate cell migration and/or differentiation (20, 36, 39, 44). Although the exact cellular function of Neph1 is unclear, studies of cell systems suggest that the phosphorylation of Neph1 induces the assembly and regulation of actin polymerization at the cell membrane. Moreover, the genetic deletion of Neph1 induces podocyte effacement, suggesting that Neph1 is involved in regulating actin cytoskeletal dynamics required for foot process formation in podocytes. The identification of Myo1c as a Neph1 binding protein and its colocalization with Neph1 in podocyte actin-rich structures support that Myo1c participates in the Neph1-dependent actin cytoskeletal dynamics of podocytes. Indeed, the requirement of an intact actin cytoskeleton for Neph1 localization (Fig. 5A and B) supports a role for Myo1c in the translocation of Neph1 to the cell membrane. We further demonstrate that alterations to the actin cytoskeleton induced by glomerular injury also induce dynamic changes to the Neph1-Myo1c complex (Fig. 5C and D). The Neph1 complex with nephrin and ZO-1 was shown previously to undergo similar dynamic changes in response to glomerular injury (8, 34, 47, 49). Therefore, it is likely that Myo1c is a functional component of a multimolecular Neph1 complex that participates in the regulation of podocyte structure and function.

A number of proteins, including actin, calmodulin, Nemo, Rictor, and the transporter protein Glut4, have been shown to associate with Myo1c (5, 30). Among these, the binding of Myo1c to Glut4 and Nemo was shown to regulate the translocation of these proteins to the cell membrane. In agreement with those findings, our results also support a role for Myo1c in the translocation of Neph1 to the podocyte cell membrane. While the translocation of Nemo and Glut4 to the plasma membrane of cultured adipocytes by Myo1c requires insulin, the localization of Neph1 at the podocyte cell membrane was stimulus independent. In our experiments the knockdown of Myo1c resulted in a significant shift of Neph1 away from the podocyte cell membrane that did not require stimulus or injury to podocytes. While this may represent an inhibition of Neph1 recycling resulting in accumulation in a cytoplasmic location, further research is needed to understand Neph1 trafficking. Myo1c is known to also mediate the localization of lipid rafts to the cell membrane (3). Since Myo1c and Neph1 both localized in lipid rafts, it is likely that the translocation of the Neph1 complex is mediated through lipid rafts associated with Myo1c. We further demonstrate that nephrin, which exists in a high-affinity complex with Neph1 and whose loss also results in podocyte effacement and renal dysfunction, also interacts with Myo1c independent of Neph1. Unlike Neph1 and nephrin, the transfection of mutant Myo1c or the depletion of Myo1c by shRNA had no effect on the localization of ZO-1 that binds

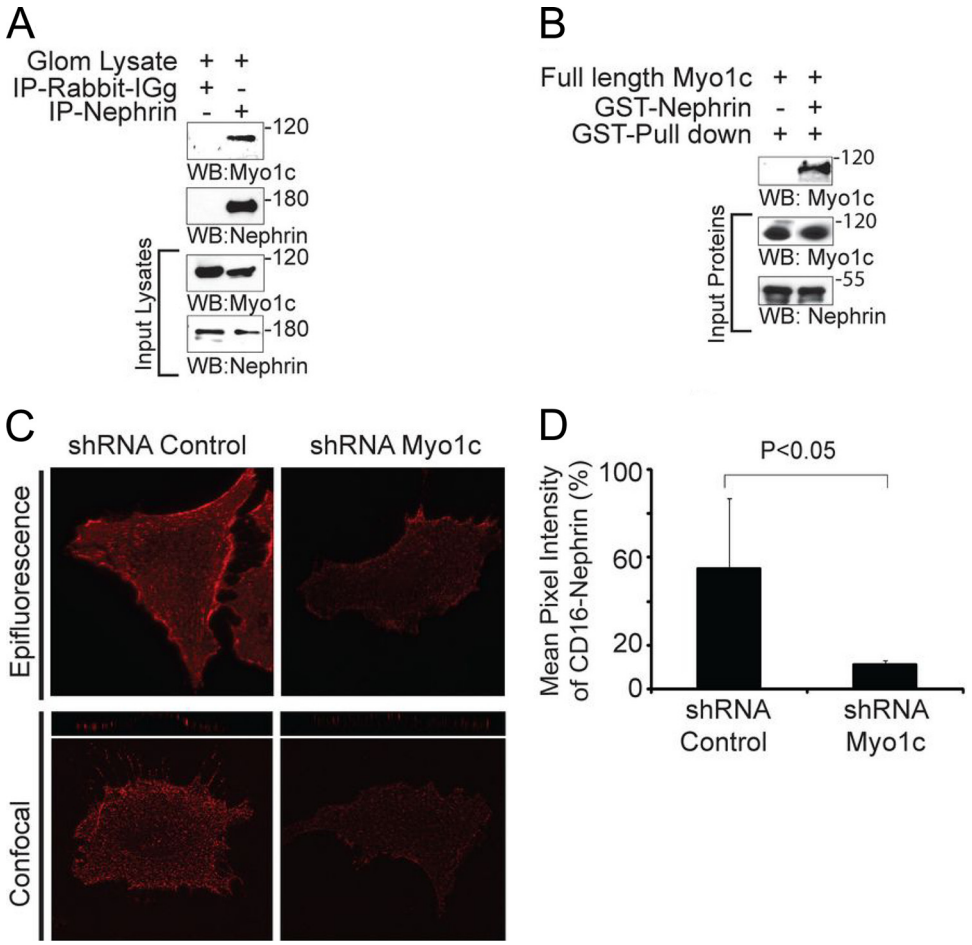

FIG. 10. Myo1c interacts with nephrin. (A) Nephrin was immunoprecipitated from glomerulus (Glom) lysates using nephrin antibody and Western blotted with Myo1c and nephrin antibodies to determine the interaction between nephrin and Myo1c. (B) A GST pulldown was performed with the cytoplasmic domain of nephrin expressed as a GST fusion protein mixed with baculovirus-expressed and purified full-length His-Myo1c, and Western blotting was performed with Myo1c antibody. (C) Myo1c knockdown and control cells were infected with retroviruses encoding CD16-nephrin. Live cells were processed for clustering with the CD16 antibody and analyzed by immunofluorescence. (D) Quantitative analysis of transfected cells ($n = 10$ cells) suggests a significant decrease in the mean pixel intensity of CD16-nephrin in Myo1c knockdown cells compared to control cells.

Neph1 and localizes at the slit diaphragm, suggesting the specificity of Myo1c for Neph1 and nephrin in this system (Fig. 6C and 7H). The requirement of Myo1c for the localization of nephrin to the podocyte cell membrane similarly to Neph1 suggests a common molecular motor-based mechanism utilized by these slit diaphragm proteins to translocate to their functional sites in podocytes.

Previously reported studies of Myo1c in diverse systems suggested that it may function as an anchor protein, providing a link between the actin cytoskeleton and cell membrane (21, 26, 33, 43). Previously reported studies also showed that Myo1c is actively involved in the membrane translocation of ion channels and their transduction complexes in stereocilia in vestibular hair cells of the ear (13). Actin-rich stereocilia are connected through extracellular filaments composed of cadherin repeats containing the proteins CDH23 and PCDH15, commonly referred as "tip links," that are critical for the adaptation response. Evidences show that Myo1c connects the transduction complex to the actin bundle and mediates the movement of this complex during adaptation and recovery events in these stereocilia. Unlike stereocilia, the foot processes of podocytes are connected through the slit diaphragm, whose molecular composition resembles that of the tip link. Similarly to tip links, the slit diaphragm contains another cadherin repeat-containing protein, FAT1, that provides structural integrity to the slit diaphragm in conjunction with the extracellular domains of Neph1 and nephrin (20, 44). Nephrin and Neph1 are connected to the actin cytoskeleton of podocytes through interactions mediated by their cytoplasmic domain (2, 10). A number of proteins have now been reported to be part of this complex, including Nck, Grb2, ZO-1, Fyn, and Par3 (15, 36). With the identification of Myo1c as a component of this complex, it is likely that, similar to stereocilia, Myo1c functions in the transduction of this complex during various physiological events in podocytes. Indeed, our knockdown and CD16 experiments, where the localization of Neph1 and nephrin at the podocyte cell membrane was significantly altered, provide support for this hypothesis. Further evidence for the

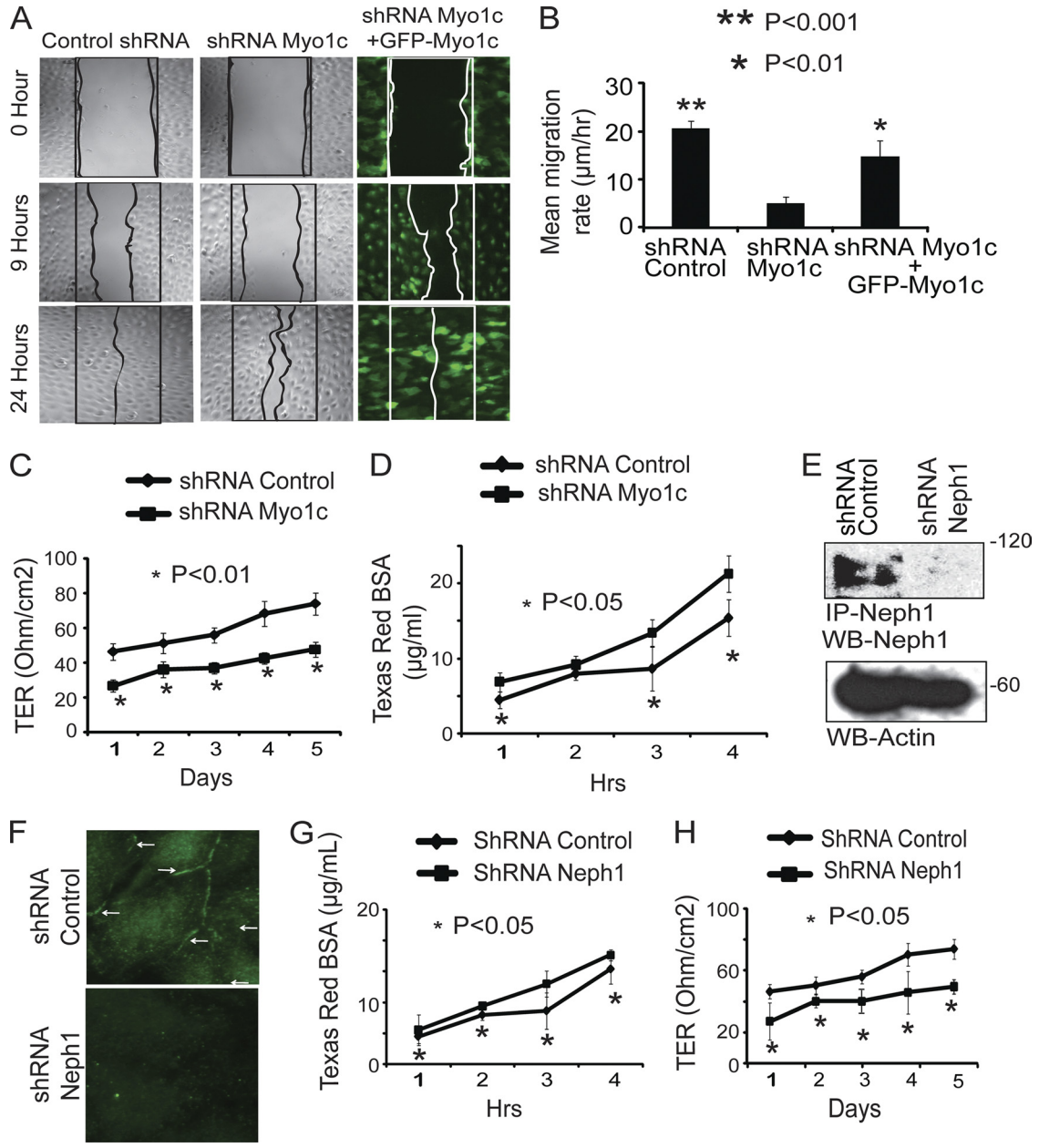

FIG. 11. Depletion of Myo1c in podocytes results in decreased cell migration, reduced TER, and increased permeability for BSA. (A) A wound assay was performed with control cells, Myo1c knockdown podocytes, and Myo1c knockdown podocytes rescued with mouse GFP-Myo1c cDNA. Wound closure was observed at different time points (only data for 0 h, 9 h, and 24 h are presented). Unlike Myo1c knockdown cells, control and rescued cells showed complete wound closure in 24 h. (B) Quantitative analysis shows a significant reduction in the mean rate of migration of knockdown cells compared to control cells ($P < 0.001$) and rescued cells ($P < 0.01$). (C) Myo1c knockdown and control podocyte cells were grown on Transwell filters, and electrical resistance was measured. Myo1c knockdown cells showed reduced TER compared to that of controls ($P < 0.05$). (D) Control and Myo1c knockdown cells grown on Transwell filters were subjected to a paracellular albumin flux assay using Texas Red-labeled albumin. Increased albumin flux over time was observed for Myo1c knockdown podocytes compared to control cells ($P < 0.05$). (E and F) A plasmid encoding Neph1 shRNA was used to generate stable Neph1 knockdown cells, and the knockdown was assessed by immunoprecipitation and Western blotting (E) and immunostaining (F). (G and H) Similarly to Myo1c knockdown cells, albumin flux and TER analyses of Neph1 knockdown cells showed increases in albumin influx (G) and reductions in the TER (H) in Neph1 knockdown cells compared to controls ($P < 0.05$).

involvement of Myo1c in the activation of Neph1 and nephrin is provided by the CD16 model system, where the knockdown of Myo1c inhibited the clustering of Neph1 and nephrin at the podocyte cell membrane. The clustering of Neph1 and nephrin also induces the activation of these proteins and the recruitment of the adapter proteins Grb2 and Nck, respectively (10, 45). Therefore, it is likely that the intracellular signaling of Neph1 and nephrin is also impaired in this model system.

Several studies now indicate that Neph1 and nephrin in

podocytes serve multiple functions involving podocyte development and junction formation that are critical for podocyte function as a filtration unit (29, 31). The engagement of the extracellular domains of Neph1 and nephrin at the podocyte cell membrane forms the structural framework of the slit diaphragm that bridges the foot processes of podocytes and is critical for podocyte function (36, 44). Therefore, to maintain the structural and functional integrity of podocytes, Neph1 and nephrin need to be localized at the podocyte membrane. Since Myo1c alters the membrane localization of Neph1 and nephrin, it is likely that the loss of Myo1c has a profound effect on podocyte function. Indeed, podocytes deficient in Myo1c had lower rates of migration in the wound assay. Moreover, their ability to form tight junctions was also impaired, as demonstrated by the TER measurements and albumin flux assay. Interestingly, similar results were obtained when Neph1 was depleted in these podocytes using Neph1-specific shRNA (Fig. 11E to H), suggesting that Neph1 and Myo1c are components of the same pathway. Collectively, these results suggest a critical role for Myo1c in podocyte function. Although many members of the myosin I family are expressed in podocytes (Fig. 1D), results from the genetic deletion of Myo1e in podocytes suggest that the function of Myo1e cannot be complemented by other myosins. The induction of podocyte effacement and proteinuria in mice with podocyte-specific Myo1e deleted indicates that members of this family are critical for maintaining podocyte function. However, the determination of the exact *in vivo* functional significance of Myo1c will require the specific deletion of this protein in podocytes. Since Neph1 and nephrin are critical for the maintenance of glomerular function, it is likely that regulating the dynamics of Neph1 and nephrin and their complex will affect the outcomes of glomerular diseases. We believe that the identification of Myo1c is a first step toward an understanding of the mechanisms that induce dynamic changes in Neph1 and nephrin distributions.

ACKNOWLEDGMENTS

This work was supported by NIDDK-sponsored grants K01 DK072047-03 and 5K01DK072047-04 and grant 1R01DK087956 and Dialysis Clinic Inc. C-2887 to D.N. Support for B.G. was provided by the German Research Foundation (GE 2158/1-1).

We thank Lawrence Holzman and Michael Ostap for their comments and suggestions.

REFERENCES

1. **Bahler, M., and A. Rhoads.** 2002. Calmodulin signaling via the IQ motif. FEBS Lett. **513:**107–113.
2. **Barletta, G. M., I. A. Kovari, R. K. Verma, D. Kerjaschki, and L. B. Holzman.** 2003. Nephrin and Neph1 co-localize at the podocyte foot process intercellular junction and form cis hetero-oligomers. J. Biol. Chem. **278:** 19266–19271.
3. **Barylko, B., G. Jung, and J. P. Albanesi.** 2005. Structure, function, and regulation of myosin 1C. Acta Biochim. Pol. **52:**373–380.
4. **Benzing, T.** 2004. Signaling at the slit diaphragm. J. Am. Soc. Nephrol. **15:**1382–1391.
5. **Bose, A., et al.** 2002. Glucose transporter recycling in response to insulin is facilitated by myosin Myo1c. Nature **420:**821–824.
6. **Coluccio, L. M.** 1997. Myosin I. Am. J. Physiol. **273:**C347–C359.
7. **Donoviel, D. B., et al.** 2001. Proteinuria and perinatal lethality in mice lacking NEPH1, a novel protein with homology to NEPHRIN. Mol. Cell. Biol. **21:**4829–4836.
8. **Doublier, S., et al.** 2001. Nephrin redistribution on podocytes is a potential mechanism for proteinuria in patients with primary acquired nephrotic syndrome. Am. J. Pathol. **158:**1723–1731.
9. **Fath, K. R., and D. R. Burgess.** 1993. Golgi-derived vesicles from developing epithelial cells bind actin filaments and possess myosin-I as a cytoplasmically oriented peripheral membrane protein. J. Cell Biol. **120:**117–127.
10. **Garg, P., R. Verma, D. Nihalani, D. B. Johnstone, and L. B. Holzman.** 2007. Neph1 cooperates with Nephrin to transduce a signal that induces actin polymerization. Mol. Cell. Biol. **27:**8698–8712.
11. **Gerke, P., T. B. Huber, L. Sellin, T. Benzing, and G. Walz.** 2003. Homodimerization and heterodimerization of the glomerular podocyte proteins nephrin and NEPH1. J. Am. Soc. Nephrol. **14:**918–926.
12. **Gillespie, P. G., et al.** 2001. Myosin-I nomenclature. J. Cell Biol. **155:**703–704.
13. **Gillespie, P. G., and J. L. Cyr.** 2004. Myosin-1c, the hair cell's adaptation motor. Annu. Rev. Physiol. **66:**521–545.
14. **Gillespie, P. G., M. C. Wagner, and A. J. Hudspeth.** 1993. Identification of a 120 kd hair-bundle myosin located near stereociliary tips. Neuron **11:**581–594.
15. **Hartleben, B., et al.** 2008. Neph-Nephrin proteins bind the Par3-Par6-atypical protein kinase C (aPKC) complex to regulate podocyte cell polarity. J. Biol. Chem. **283:**23033–23038.
16. **Heintzelman, M. B., T. Hasson, and M. S. Mooseker.** 1994. Multiple unconventional myosin domains of the intestinal brush border cytoskeleton. J. Cell Sci. **107**(Pt. 12)**:**3535–3543.
17. **Holt, J. R., et al.** 2002. A chemical-genetic strategy implicates myosin-1c in adaptation by hair cells. Cell **108:**371–381.
18. **Holzman, L. B., et al.** 1999. Nephrin localizes to the slit pore of the glomerular epithelial cell. Kidney Int. **56:**1481–1491.
19. **Huber, T. B., et al.** 2003. The carboxyl terminus of Neph family members binds to the PDZ domain protein zonula occludens-1. J. Biol. Chem. **278:** 13417–13421.
20. **Johnstone, D. B., and L. B. Holzman.** 2006. Clinical impact of research on the podocyte slit diaphragm. Nat. Clin. Pract. Nephrol. **2:**271–282.
21. **Jung, G., K. Remmert, X. Wu, J. M. Volosky, and J. A. Hammer III.** 2001. The Dictyostelium CARMIL protein links capping protein and the Arp2/3 complex to type I myosins through their SH3 domains. J. Cell Biol. **153:** 1479–1497.
22. **Kwon, O., C. L. Phillips, and B. A. Molitoris.** 2002. Ischemia induces alterations in actin filaments in renal vascular smooth muscle cells. Am. J. Physiol. Renal Physiol. **282:**F1012–F1019.
23. **Lambert, J., J. M. Naeyaert, T. Callens, A. De Paepe, and L. Messiaen.** 1998. Human myosin V gene produces different transcripts in a cell type-specific manner. Biochem. Biophys. Res. Commun. **252:**329–333.
24. **Liu, G., et al.** 2003. Neph1 and nephrin interaction in the slit diaphragm is an important determinant of glomerular permeability. J. Clin. Invest. **112:** 209–221.
25. **Lowenborg, E. K., G. Jaremko, and U. B. Berg.** 2000. Glomerular function and morphology in puromycin aminonucleoside nephropathy in rats. Nephrol. Dial. Transplant. **15:**1547–1555.
26. **Manceva, S., et al.** 2007. Calcium regulation of calmodulin binding to and dissociation from the myo1c regulatory domain. Biochemistry **46:**11718–11726.
27. **Marshall, C. B., J. W. Pippin, R. D. Krofft, and S. J. Shankland.** 2006. Puromycin aminonucleoside induces oxidant-dependent DNA damage in podocytes in vitro and in vivo. Kidney Int. **70:**1962–1973.
28. **McConnell, R. E., and M. J. Tyska.** 2010. Leveraging the membrane-cytoskeleton interface with myosin-1. Trends Cell Biol. **20:**418–426.
29. **Moreno, J. A., et al.** 2008. A slit in podocyte death. Curr. Med. Chem. **15:**1645–1654.
30. **Nakamori, Y., et al.** 2006. Myosin motor Myo1c and its receptor NEMO/IKK-gamma promote TNF-alpha-induced serine307 phosphorylation of IRS-1. J. Cell Biol. **173:**665–671.
31. **Neumann-Haefelin, E., et al.** 2010. A model organism approach: defining the role of Neph proteins as regulators of neuron and kidney morphogenesis. Hum. Mol. Genet. **19:**2347–2359.
32. **Nihalani, D., H. Wong, R. Verma, and L. B. Holzman.** 2007. Src family kinases directly regulate JIP1 module dynamics and activation. Mol. Cell. Biol. **27:**2431–2441.
33. **Novak, K. D., and M. A. Titus.** 1998. The myosin I SH3 domain and TEDS rule phosphorylation site are required for in vivo function. Mol. Biol. Cell **9:**75–88.
34. **Otaki, Y., et al.** 2008. Dissociation of NEPH1 from nephrin is involved in development of a rat model of focal segmental glomerulosclerosis. Am. J. Physiol. Renal Physiol. **295:**F1376–F1387.
35. **Patari-Sampo, A., P. Ihalmo, and H. Holthofer.** 2006. Molecular basis of the glomerular filtration: nephrin and the emerging protein complex at the podocyte slit diaphragm. Ann. Med. **38:**483–492.
36. **Patrakka, J., and K. Tryggvason.** 2010. Molecular make-up of the glomerular filtration barrier. Biochem. Biophys. Res. Commun. **396:**164–169.
37. **Patrakka, J., and K. Tryggvason.** 2007. Nephrin—a unique structural and signaling protein of the kidney filter. Trends Mol. Med. **13:**396–403.
38. **Pierchala, B. A., M. R. Munoz, and C. C. Tsui.** 2010. Proteomic analysis of the slit diaphragm complex: CLIC5 is a protein critical for podocyte morphology and function. Kidney Int. **78:**868–882.
39. **Saleem, M. A., et al.** 2002. Co-localization of nephrin, podocin, and the actin cytoskeleton: evidence for a role in podocyte foot process formation. Am. J. Pathol. **161:**1459–1466.

40. **Sellin, L., et al.** 2003. NEPH1 defines a novel family of podocin interacting proteins. FASEB J. **17:**115–117.
41. **Shankland, S. J.** 2006. The podocyte's response to injury: role in proteinuria and glomerulosclerosis. Kidney Int. **69:**2131–2147.
42. **Swiatecka-Urban, A., et al.** 2004. Myosin VI regulates endocytosis of the cystic fibrosis transmembrane conductance regulator. J. Biol. Chem. **279:** 38025–38031.
43. **Tang, N., T. Lin, and E. M. Ostap.** 2002. Dynamics of myo1c (myosin-ibeta) lipid binding and dissociation. J. Biol. Chem. **277:**42763–42768.
44. **Tryggvason, K., T. Pikkarainen, and J. Patrakka.** 2006. Nck links nephrin to actin in kidney podocytes. Cell **125:**221–224.
45. **Verma, R., et al.** 2006. Nephrin ectodomain engagement results in Src kinase activation, nephrin phosphorylation, Nck recruitment, and actin polymerization. J. Clin. Invest. **116:**1346–1359.
46. **Wagner, M. C., B. Barylko, and J. P. Albanesi.** 1992. Tissue distribution and subcellular localization of mammalian myosin I. J. Cell Biol. **119:**163–170.
47. **Wagner, M. C., et al.** 2008. Ischemic injury to kidney induces glomerular podocyte effacement and dissociation of slit diaphragm proteins Neph1 and ZO-1. J. Biol. Chem. **283:**35579–35589.
48. **Wang, L., et al.** 2005. Activation of Galpha q-coupled signaling pathways in glomerular podocytes promotes renal injury. J. Am. Soc. Nephrol. **16:**3611–3622.
49. **Wernerson, A., et al.** 2003. Altered ultrastructural distribution of nephrin in minimal change nephrotic syndrome. Nephrol. Dial. Transplant. **18:**70–76.
50. **Yip, M. F., et al.** 2008. CaMKII-mediated phosphorylation of the myosin motor Myo1c is required for insulin-stimulated GLUT4 translocation in adipocytes. Cell Metab. **8:**384–398.